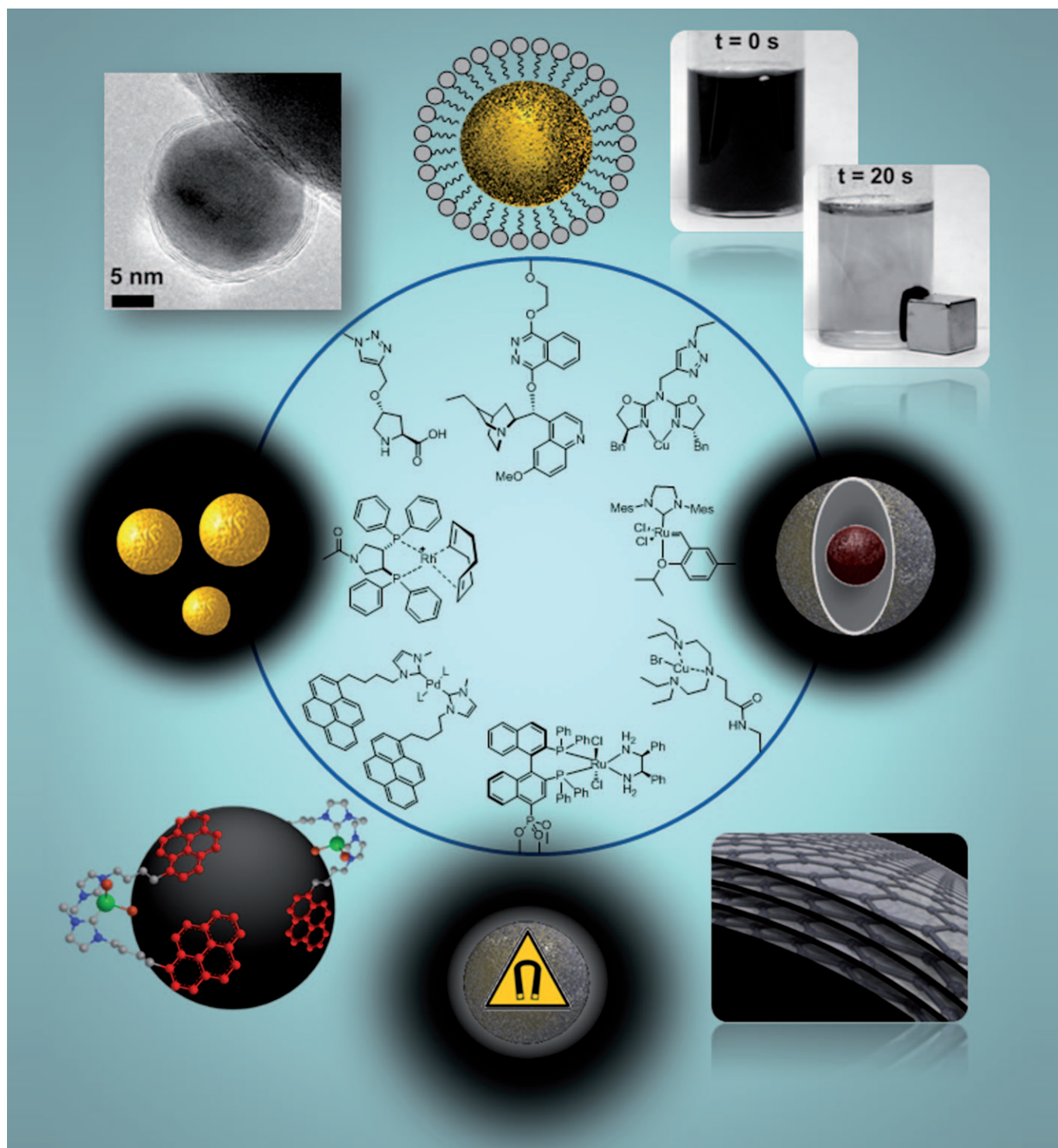


## Nanoparticles as Semi-Heterogeneous Catalyst Supports

Alexander Schätz,<sup>[a, b]</sup> Oliver Reiser,<sup>[b]</sup> and Wendelin J. Stark<sup>✉[a]</sup>



**Abstract:** Nanoparticles can serve as semi-heterogeneous supports since they readily disperse in common solvents and combine high surface area with excellent accessibility. Reversible agglomeration through solvent changes and magnetic separation provide technically attractive alterna-

tives to classical catalyst filtration. This account places emphasis on recent developments in this emerging area.

**Keywords:** colloids • gold • heterogeneous catalysis • immobilization • magnetic nanoparticles • nanocatalysis

## Introduction

Catalysis is among the most important applications within the field of nanoscience.<sup>[1]</sup> Next to oxide supports, the large surface area of metal nanoparticles, the only scaffold that shall be discussed in this Review, qualifies them quite naturally to act either as heterogeneous promoters for catalytic reactions or as a support for homogeneous catalysts.<sup>[2]</sup> This Review discusses how spherical particles provide attractive supports for catalysis with other non-traditional properties. Contrary to classic heterogeneous catalysts,<sup>[3]</sup> nanoparticles (NPs) are typically synthesized in a bottom-up approach from molecular precursors such as a metal salt, a stabilizer, and a reducing agent (with the latter two being sometimes identical). When catalytic applications of NPs are discussed, four general approaches can be considered in distinct form or as combinations thereof. They can be discriminated in terms of the role of the metal the nanoparticle consists of, the location of the ligand, if any, with respect to the particle surface, and whether the ligand plays an active part in the catalytic process or acts solely as a stabilizer.

Even more complex morphologies are possible if bimetallic nanoparticles or multilayer shells are considered. The first three approaches involve the use of systems in which the nanoparticle metal exerts the dominating influence on the catalytic activity (Figure 1 a–c). In all these cases, the catalytic processes take place on the surface of the nanoparticles, affected only in one structure by ligands/capping agents that transmit influence to metal-coordinated substrates in their vicinity (Figure 1 c). A plethora of clusters with constituent metals such as Pt, Pd, Ru, and Rh has been reported.<sup>[4]</sup> Since the catalytic properties of these metal nanoparticles, which act in principle as heterogeneous catalysts, have been extensively reviewed,<sup>[2]</sup> the following chapters will focus on the emerging field of nanomaterials acting

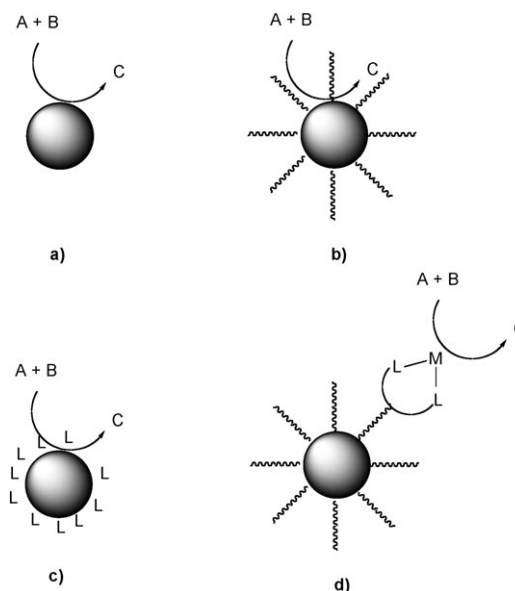


Figure 1. Catalysis with a) metal nanoparticles, b) metal nanoparticles capped with a protective shell, c) metal nanoparticles capped with ligands contributing to the catalytic activity, and d) metal nanoparticles with catalysts supported on the protective shell. Only in the last case the core material does not promote the reaction.

solely as carriers for soluble catalysts (Figure 1 d), an approach that has been scarcely discussed.<sup>[5]</sup> In this case, the clusters act as a structuring element for an assembly of ligands, which are bonded to the core material through an additional function, different from the chelating functional groups that define the catalytic center. Importantly, the catalytic activity does not arise from the core material.

For these nanoclusters, catalysts are exposed on the particle surface, which makes them accessible almost like their homogeneous counterparts. Such a globular surface might be superior to conventional polymeric supports, which represent the most popular scaffolds used for immobilization to date.<sup>[6]</sup> Amorphous resins sometimes have the problem that catalytic sites are buried in the polymer backbone, thus limiting the access of reactants.<sup>[7]</sup> This limitation was widely tolerated since the benefits from grafting of an otherwise soluble heavy-metal complex or organocatalyst, namely ease of separation and recyclability of the usually toxic and expensive species, outweigh the loss of activity and selectivity occasionally observed. Soluble transition-metal complexes, in

[a] Dr. A. Schätz, Prof. Dr. W. J. Stark  
Institut für Chemie- und Bioingenieurwissenschaften  
Department Chemie und Angewandte Biowissenschaften  
ETH Zürich HCI E 107  
Wolfgang-Pauli-Strasse 10, 8093 Zürich (Switzerland)  
Fax: (+41)44-633-1083  
E-mail: wstark@ethz.ch

[b] Dr. A. Schätz, Prof. Dr. O. Reiser  
Institute for Organic Chemistry, University of Regensburg  
Universitätsstrasse 31, 93053 Regensburg (Germany)  
Fax: (+49)941-943-4121

particular, are difficult to separate, a fact which has limited their application in large-scale pharmaceutical processes due to metal contamination.<sup>[8]</sup> Furthermore, the separation of heterogeneous matrices from a reaction mixture is more straightforward than separation from biphasic systems, for example, extraction using perfluorinated tags.<sup>[9]</sup> The domain of nanoparticles acting as a recyclable scaffold lies between these two orthogonal strategies, hence, this approach is sometimes called “semi-heterogeneous”.<sup>[2f]</sup> The separation of the functionalized nanomaterial can be achieved by different methods, such as centrifugation, precipitation–floculation, nanofiltration, or magnetic decantation (in the case of magnetic nanoparticles), depending on the nature of the particles.

---

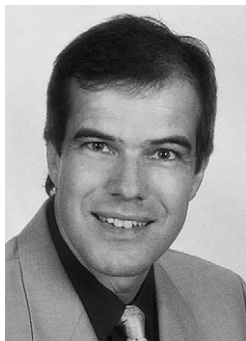


---

Alexander Schätz, born in 1979, studied chemistry at the University of Regensburg where he joined the group of Prof. O. Reiser for a Diploma thesis in the field of asymmetric catalysis. He received his Ph.D. within the international doctorate program NanoCat/ENB in 2009 and is currently a postdoctoral researcher in the group of Prof. W. J. Stark with interests centered in nanocatalysis.



Oliver Reiser obtained his Ph.D. 1989 in Hamburg with Prof. Armin de Meijere. Following two postdoctoral posts at the IBM research center, San Jose and Harvard University (D. A. Evans), Cambridge, USA, he moved to the University of Göttingen in 1992. After completing his habilitation in 1995, he moved to Stuttgart University as an Associate Professor in 1996, and in 1997 he was appointed as Professor of Organic Chemistry at the University of Regensburg. His research interests focus around stereoselective synthesis and catalysis towards natural products and analogues.



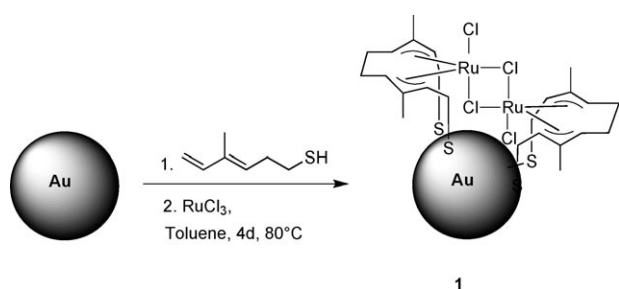
Wendelin J. Stark, born in 1976, received his Master in Chemistry in 2000 followed by a Ph.D. in Mechanical Engineering in 2002 from the ETH Zurich. He founded the Functional Materials Laboratory in 2004. He pursues application-oriented research at the interface of chemistry with material science and medicine.



Since the core material is not meant to take part in the catalytic reaction (support role only), this metal should be comparatively inactive or surrounded by a widely impermeable shell. The latter condition is rather difficult to accomplish, which explains why only a few metals have been used as structural elements, despite the many different metal NPs used in heterogeneous catalysis. Therefore, gold colloids tethered to a protective alkanethiol-monolayer were for a long time the dominating motif for nanosized core–shell structures.<sup>[10]</sup> They profited from the ease of preparation and the “inertness” of Au<sup>0</sup>, an assumption which is, however, not completely true.<sup>[11]</sup> Progress in the synthesis of stable magnetic nanoparticles has fuelled the number of possible applications, such as magnetic storage media,<sup>[12]</sup> vessels for drug delivery<sup>[13]</sup> and cancer treatment through hyperthermia<sup>[14]</sup> as well as contrast agents for magnetic resonance imaging (MRI),<sup>[15]</sup> thus suggesting their use as a catalyst support. The advantage over gold colloids lies in their physical and chemical stability, which is highly dependent on the nature of the protecting shell, and clearly in the ease of separation by using an external magnet. Hence, the categories of different nanoparticle supports will be classified by the nature of the metal core and coating rather than the immobilized catalyst or the promoted reaction.

### Monolayer-Protected Gold Clusters

The first nanosized core–shell structures utilized as supports for catalysts were gold colloids. Au nanoclusters sufficiently stable to act as supports for metal complexes usually feature a stabilizing alkanethiol monolayer on which the catalysts are anchored. The exceptional stability of the Au–S bond could result in a misguided association of a certain rigidity of the shell. In fact, the self-assembling monolayer (SAM) on the particle surface is far more comparable to a two-dimensional fluid in terms of its behavior. Thiolates constantly shift on the cluster, “hopping”<sup>[16]</sup> from one cluster to the next, or exchanging with thiols occasionally present in the supernatant. The latter behavior offers a straightforward route for the attachment of functionalized thiols via the so-called place-exchange reaction.<sup>[17]</sup> Early studies feature examples of an in situ functionalization by passivation of preformed gold colloids or simultaneously to the growth of gold nuclei, which form upon reduction of tetrachloroaurate with sodium borohydride according to a procedure developed by Brust, Schiffrin et al.<sup>[18]</sup> Owing to the exceptionally simple and concise layout of the Schiffrin reaction, chemistry using monolayer-protected gold clusters (AuMPCs) proved very popular.<sup>[19]</sup> The first transition-metal complex immobilized on metal nanoparticles was reported by Tremel et al. in 1998.<sup>[20]</sup> Freshly prepared gold colloids were stirred with 4-methylhexa-3,5-diene-1-thiol in the presence of RuCl<sub>3</sub> under argon to yield a black powder, which could be dissolved in acetone and precipitated from methanol (Scheme 1). The gold-grafted Ru complex **1** was able to catalyze the ring-opening metathesis polymerization

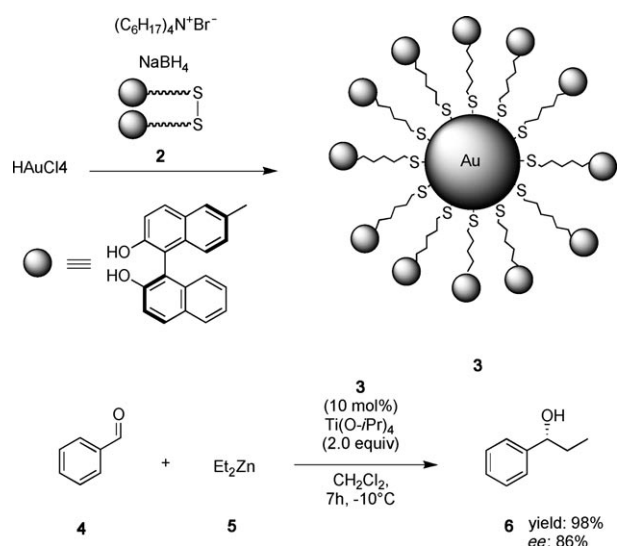


Scheme 1. Tagging of gold colloids with a Ru complex for the ring-opening metathesis polymerization (ROMP) of norbornene to polynorbornene.

(ROMP) of norbornene, providing turnover frequencies (TOF:  $16000\text{ h}^{-1}$ ) superior to those obtained with the homogeneous counterpart (TOF:  $3000\text{ h}^{-1}$ ). It was reasoned that the orientation of the catalyst on the surface of the MPCs favors the coordination of the monomer and the orientation of the growing polymer chain. However, turnover frequencies of Ru complexes on two-dimensional Au surfaces even far exceeded the values obtained with their three-dimensional counterparts (TOF:  $80000\text{ h}^{-1}$ ).

In elegant studies, Sasai et al.<sup>[21]</sup> reported on Au clusters stabilized by thiols bearing chiral 1,1'-bi-2-naphthol (BINOL) moieties by using exclusively disulfides with (*R*)-BINOL at the terminal position. Since functionalized disulfides were employed already during the Schiffrin reaction, core passivation and functionalization succeeded in a one-pot reaction that makes this route comparatively simple. A Ti-BINOLate complex was able to catalyze the asymmetric alkylation of benzaldehyde using  $\text{Et}_2\text{Zn}$  in up to 98% yield and with 86% *ee* (Scheme 2).

BINOL-functionalized MPCs **3** gave results comparable to the homogeneous catalyst (95% yield, 90% *ee*) and clear-



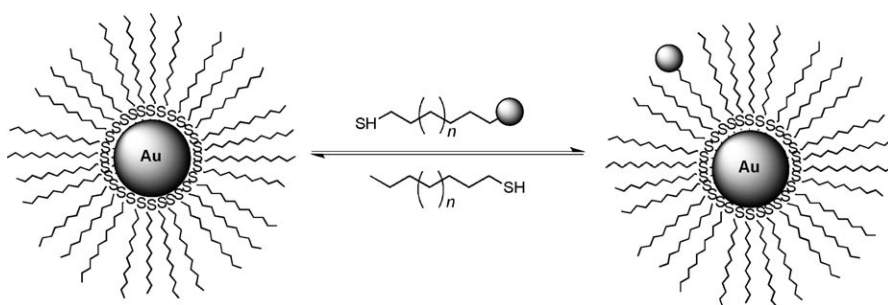
Scheme 2. In situ synthesis of Ti-BINOLated-AuMPCs (top) and asymmetric alkylation of benzaldehyde (**4**) with diethylzinc (**5**) catalyzed by **3** (bottom).

ly superior to polystyrene-supported Ti-BINOLate complexes (61% yield, 83% *ee*).<sup>[21c]</sup> A specific advantage of thiolated gold colloids lies in their agglomeration behavior, which allows their rapid precipitation from polar, and re-dispersion in apolar solvents. Thus, recycling of the nanocomposite was possible by precipitation from EtOH and redispersion in  $\text{CH}_2\text{Cl}_2$ , although this procedure was accompanied by a notable drop in enantioselectivity (62% *ee*). In addition, the length of the alkanethiol spacer ( $\text{C}_4$ ,  $\text{C}_5$ ,  $\text{C}_6$ ) was found to have quite an effect on the selectivity in the alkylation of several aldehydes. Albeit such an in-situ functionalization is very appealing, its scope is limited to rather insensitive ligand precatalysts, given the fact that the Schiffrin reaction demands harsh reductive conditions. However, Sasai et al. expanded this concept to immobilizing multicomponent asymmetric catalysts such as Ga-Na-bis(binaphthoxide) complexes.<sup>[21b]</sup> The synthesis was akin to the one depicted in Scheme 2, using methoxymethyl(MOM)-protected BINOL-terminated disulfides but with a significantly longer ( $\text{C}_{16}$ ) alkyl spacer. The as-prepared AuMPC-supported BINOL (20 mol%) was treated with  $\text{GaCl}_3$  (20 mol%) and  $\text{NaOtBu}$  (85 mol%) in the presence of cyclohex-2-enone and dibenzylmalonate to afford the corresponding Michael adduct in 98% *ee*, which is comparable to the parent homogeneous catalyst. In this regard, the work by Gao et al.<sup>[5]</sup> is worthy of note. They designed a maghemite-supported Ti-BINOLate complex, which was envisaged to deliver results comparable to the AuNP-based catalyst **3** developed by Sasai et al. Surprisingly, under conditions similar to those depicted in Scheme 2, only moderate reaction yields (47–55%) and enantioselectivities (15–43% *ee*) were achieved.

### Gold Nanoparticles with Mixed Monolayers

In contrast to the aforementioned in situ preparation strategies, the exchange of surface-bound thiolates for dissolved functionalized thiols represents a convenient post-grafting process (Scheme 3).

The place-exchange reaction of thiolates on 3D surfaces, such as AuNPs, has been studied extensively.<sup>[17]</sup> In general, the tendency of thiolates ligating gold clusters to exchange with thiols in the supernatant is higher than on 2D surfaces. Whereas terrace sites are the predominant motif on a flat Au(111) surface, the core surfaces of nanoclusters<sup>[22]</sup> contain a large fraction of classically defined defect sites. The different surface sites exhibit a substantial gradation in reactivity. Thiolates on vertexes and edges are significantly easier to exchange than the ones on the interior terrace sites.<sup>[17f]</sup> Evidence was found for both associative<sup>[17f,23]</sup> ( $\text{S}_\text{N}2$ -like) and dissociative ( $\text{S}_\text{N}1$ -like)<sup>[17i,24]</sup> pathways as the rate-determining step. Reaction kinetics were represented satisfactorily in a pseudo-first-order process.<sup>[17j]</sup> In an associative pathway, the thiol enters the monolayer, protonates, and then substitutes a bound thiolate ligand. This process does not alter the core dimensions, hence, the size of the Au particles can be controlled prior to particle modification following well-elaborat-



Scheme 3. Place-exchange reaction of surface-bound thiolates and dissolved  $\omega$ -functionalized alkanethiols.

ed protocols, whereas the previously discussed in situ routes lack such simple size-control. The rate of place-exchange decreases with an increase in the size of the entering ligand and the chain length of the protecting monolayer.<sup>[17]</sup> However, the most significant advantage of this post-grafting procedure is the formation of mixed alkanethiol monolayers, which enables higher degrees of complexity in the SAM compared to those obtained by in situ methods. For instance, the use of alkanethiols with different chain lengths results in variably constructed catalytic sites. Complexes positioned on long-chained alkanethiols relative to the neighboring thiolates form convex reaction sites, similar to homogeneous catalysts, whereas concave reaction sites are created with short-chained thiols resembling enzyme-like environments (Figure 2).

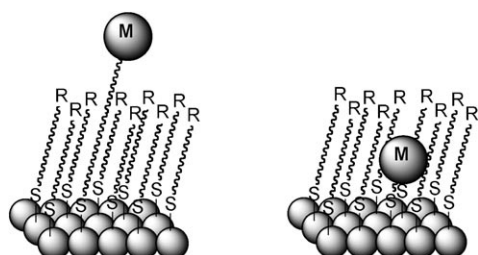
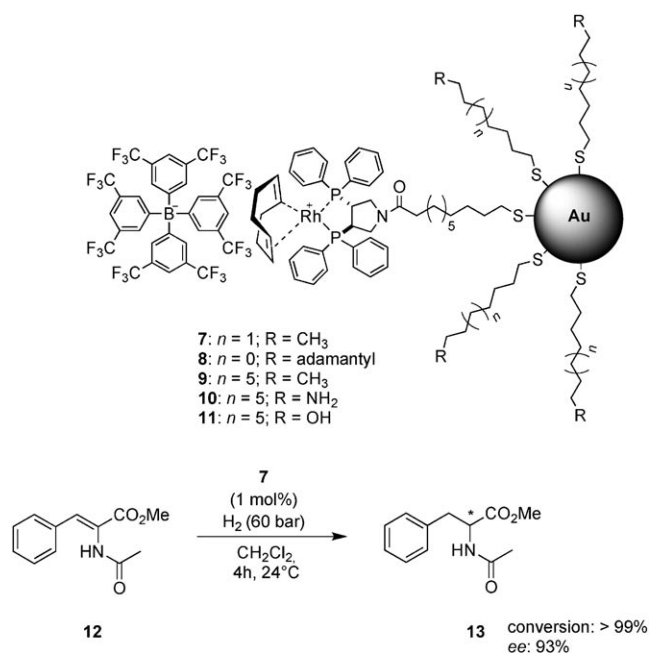


Figure 2. Different active sites for metal catalysts on thiolate monolayers: Convex active site (homogeneous-like, left) and concave active site (enzyme-like, right).

In addition, the loading of the particles can be controlled in place-exchange reactions by careful choice of concentrations and reaction times. Different termini of the surrounding alkanethiolates in the monolayer can be used to tune the solubility or reactivity of the cluster through interactions with the substrate or the catalytic center. Following this concept, Belser, Stöhr, and Pfaltz<sup>[25]</sup> have published a comprehensive study using a [Rh(cod)(PYRPHOS)]BArF catalyst. Different gold colloids were synthesized by a place-exchange reaction of AuMPCs with unequal chain lengths ( $C_6$ – $C_{12}$ ) and end group polarity of the alkanethiolates in the shell for rhodium PYRPHOS bearing thiols (Scheme 4). Almost all “heterogenized” catalysts gave yields (>99%) and enantioselectivities (93% *ee*) equal to those obtained

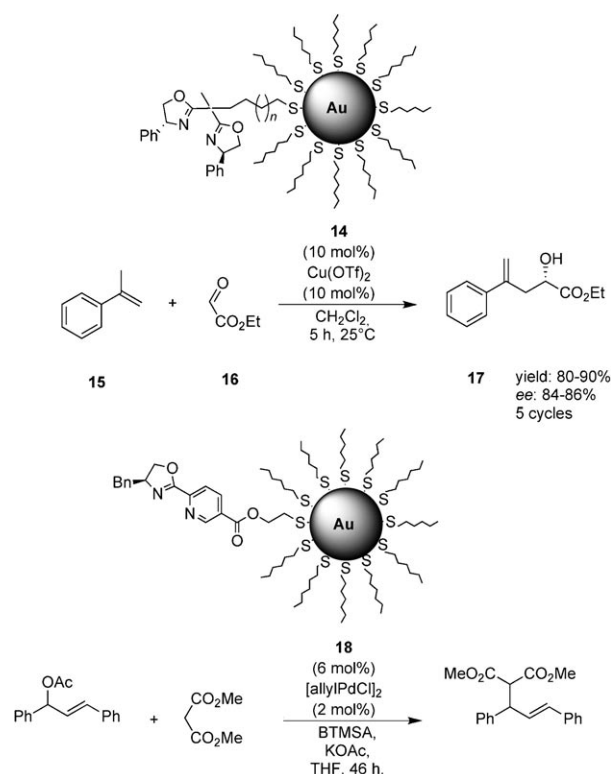
with homogeneous [Rh(cod)(*n*-octanoyl-PYRPHOS)]BArF in the hydrogenation of methyl  $\alpha$ -acetamidocinnamate **12**. The colloids could be recovered by filtration and reused at least three times without loss of enantioselectivity.

AuMPCs **10** and **11** were tethered with polar end groups to tune the solubility and reac-



Scheme 4. Asymmetric hydrogenation of methyl  $\alpha$ -acetamidocinnamate (**12**) in the presence of [Rh(cod)(PYRPHOS)]BArF-AuMPCs.

tivity of the cluster in accordance with the aforementioned principle of a controlled catalyst environment. Unfortunately, these compounds, in particular, delivered significantly lower yield (32–94%) and selectivity (82–86% *ee*). Thus, the promising strategy of creating AuNPs compatible with polar-protic reaction media was unsuccessful. The concept of forming pocket-like environments for catalysts by varying the alkyl-chain length of the linking thiol was applied in an early study by Tanaka et al.<sup>[26]</sup> and pushed to its limits by Koskinen and co-workers.<sup>[27]</sup> Both used oxazoline-based ligands incorporated in gold clusters protected by hexanethiols. Tanaka et al. examined the influence of different spacer lengths ( $C_4$ ,  $C_6$ ,  $C_8$ ,  $C_{10}$ ) of the alkanethiols linked to the central carbon atom of a chiral bis(oxazoline) on the dispersability and reactivity of the corresponding (*R*)-Ph-BOX-AuMPCs (Scheme 5, top). The copper(II) complexes of the functionalized AuMPCs **14** acted as nearly homogeneous catalysts in the ene reaction between 2-phenylpropene (**15**) and ethyl glyoxylate (**16**). It was found that ligands tethered

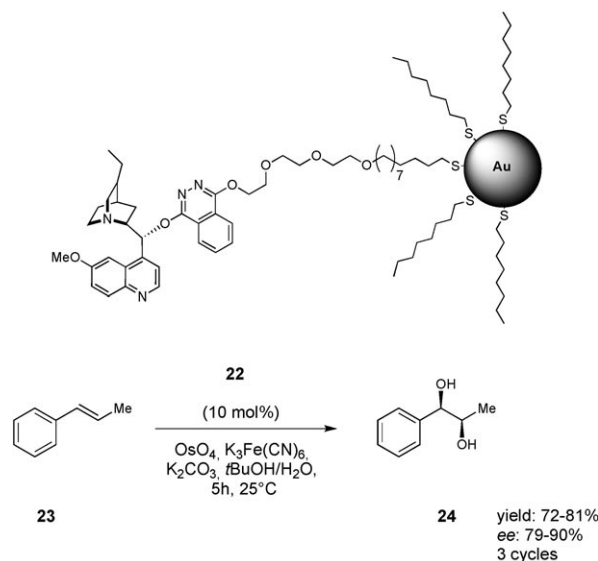


Scheme 5. Chiral oxazoline-based ligands in a concave environment within the shell of hexanthiolate-protected AuMPCs.

with the shortest ( $C_4$ ) linker show the highest level of dispersion and are the most effective in terms of catalytic activity and recycling utility. The authors reasoned that use of a concave active site with copper(II) complexes buried in the hexanthiolate-shell minimized aggregation of the particles. Albeit the recycling of these highly dispersed particles is laborious, involving shaking after dilution with hexane, centrifugation, and decantation, yields decreased only slightly from 99% to 80% in the fifth run and good enantioselectivities were achieved in each cycle (84–86% *ee*).

A chiral PyOX ligand was buried even deeper in the hexanthiolate coating of the gold particle (Scheme 5, bottom).<sup>[27]</sup> The authors suggested that a 32-atom gold cluster was formed, resembling a hollow structure, which would represent the smallest core diameter ( $1.2 \pm 0.2$  nm) ever used for AuMPCs serving as carriers for catalysts. However, the catalytic activity of the palladium complexes of these MPCs in the alkylation of chalconol acetate (**19**) with dimethyl malonate (**20**) was limited. It showed only negligible activity but slightly better enantioselectivity than a polystyrene-bound analogue. Complete conversions and selectivities up to 73% were possible with diverse homogeneous PyOX ligands, thus suggesting that an enzyme-like binding site has a detrimental effect on this reaction. A very early example for a convex active site forming a homogeneous-like environment was reported by Mrksich and co-workers.<sup>[28]</sup> In fact, this represented the first application of a chiral catalyst immobilized on AuNPs. A mixed monolayer was formed con-

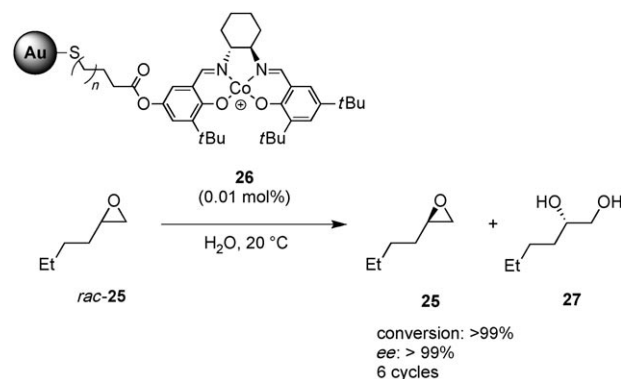
taining 25% of dihydroquinidine-functionalized alkanethiols neighboring octanethiolate on gold cores with an average diameter of 2.5 nm (Scheme 6). The chiral cinchona alkaloid



Scheme 6. Asymmetric dihydroxylation of  $\beta$ -methyl styrene **23** using cinchona alkaloid **22** tagged to gold colloids in a convex fashion.

derivative **22** was used to activate oxidant osmium tetroxide to render the Sharpless asymmetric dihydroxylation of  $\beta$ -methyl styrene (**23**) highly enantioselective (90% *ee*). It is noteworthy that **24** was sufficiently stable to allow recycling by gel permeation chromatography at least twice, thus impressively demonstrating the versatility of this support even in aqueous media and under oxidative conditions.

When it comes to recyclability, the work of Belser and Jacobsen<sup>[29]</sup> needs to be mentioned. They reported a chiral  $Co^{III}$ -salen complex grafted on octanethiolate-coated gold nanoclusters for the hydrolytic kinetic resolution of epoxides (Scheme 7). It maintained its excellent selectivity and reactivity, which was even superior to its homogeneous counterpart, in six iterative runs. The subsequent drop in activity

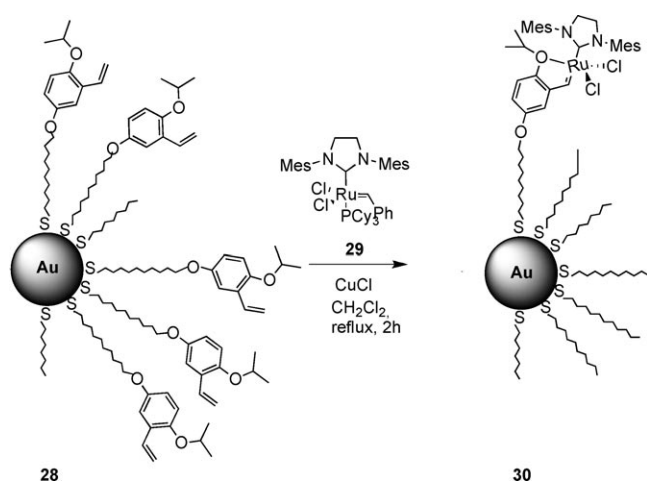


Scheme 7. Hydrolytic kinetic resolution of racemic epoxide **25** with immobilized catalyst **26**.



was due to reduction of the cobalt species rather than catalyst leaching, thus, reactivity was restored upon oxidation. A recent study carried out by Yu et al.<sup>[30]</sup> reported a similar activity enhancement for a heterogenized palladium–bipyridyl complex in alkyne cyclotrimerization reactions, which was attributed to interphase effects.

An immobilized Hoveyda–Grubbs catalyst developed by Lee et al.<sup>[31]</sup> turned out to be equally suited for several consecutive metathesis reactions. Octanethiolate-passivated AuMPCs were exchanged with styrene-functionalized dodecanethiols. Treatment of cluster **28** thus obtained with second-generation Grubbs catalyst **29** in the presence of CuCl yielded AuMPC–Ru–carbene complex **30** (Scheme 8).



Scheme 8. Synthesis of AuMPC-bound Ru-carbene complex **30** for the ring-closing metathesis of dienes.

In a very similar procedure, the selfsame catalyst was anchored on different magnetic nanoparticles.<sup>[32]</sup> Catalyst **30** proved to be soluble in CH<sub>2</sub>Cl<sub>2</sub> and was recovered by precipitation from methanol, ethanol, or diethyl ether. This material showed high reactivity (>98% conversion) in the ring-closing olefin metathesis of several dienes to heterocyclic compounds.

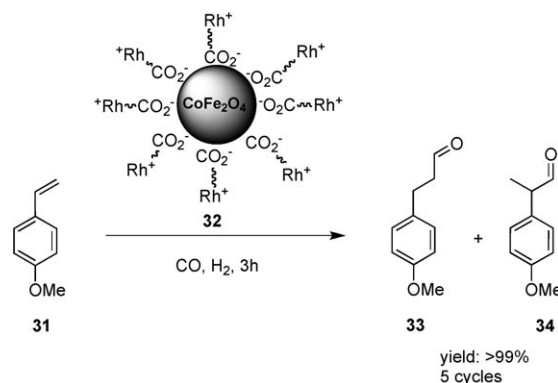
After the sixth run, conversion decreased dramatically from 80% down to 20% accompanied by particle flocculation. Desorption of the coating monolayer followed by aggregation of the gold cores might be responsible for this effect, a suspicion which was substantiated by TEM analysis. As shown in the previous examples, activities and selectivities of catalysts immobilized on gold nanoparticles reach levels that are often restricted to homogeneous catalysts and rarely equalled by complexes anchored on solid supports. This might be attributed to the excellent dispersibility of these particles, sometimes even considered “soluble”.<sup>[31]</sup> In addition, the immobilization on AuMPCs offers many prospects, such as tuning the environment of the catalytic sites. However, it has to be admitted that recycling is sometimes tedious and possible only in a limited number of cycles. After several cycles the monolayers start to desorb from the

surface of the cluster, thus causing irreversible aggregation of the gold nuclei and finally resulting in a material that cannot be dispersed anymore. Driven by the motivation to retain the beneficial properties of the AuMPCs and to simultaneously overcome limitations in recycling, especially with regard to feasibility and deficiency in number, several groups disclosed nanoparticles that contain magnetic core materials.

## Ferrite Nanoparticles

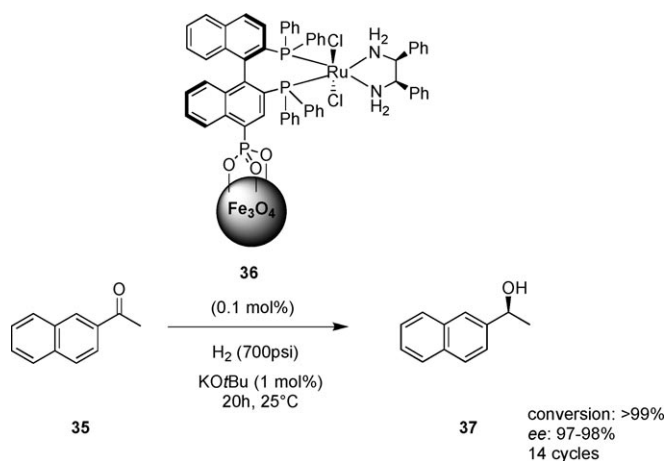
Recent advances in the synthesis of size-controlled and monodisperse magnetic ferrite nanoparticles without the call for size-selection facilitated the exploitation of these particles in many applications.<sup>[33]</sup> Similar to gold nanoparticles, these materials allow surface stabilization by simple organic compounds. Carboxylic acid sites are predominant among the most common capping agents for ferrite nanoparticles.<sup>[34]</sup> Thus, an early example for magnetic nanoparticles coated with a homogeneous catalyst is provided by a Rh-based cationic catalyst modified with benzoic acid, namely [Rh(cod)-η<sup>6</sup>-benzoic acid]BF<sub>4</sub>.<sup>[35]</sup> Co-ferrite (CoFe<sub>2</sub>O<sub>4</sub>) was chosen as support, which possesses a deviation from the nominal structure of a spinel ferrite in the shell. An amorphous ferric hydroxide layer on the surface was proposed,<sup>[36]</sup> which explained the non-stoichiometric composition. The saturation magnetization of this nanomaterial with a size distribution ranging from 8 to 20 nm was reported to be approximately 60 emu g<sup>-1</sup>. Similar to the place-exchange reaction, surface modification did not alter the chemical composition, which resulted in the form (CoFe<sub>2</sub>O<sub>4</sub>)<sub>core</sub>(Fe<sub>0.19</sub>O<sub>x</sub>)<sub>shell</sub>-{[Rh(cod)-η<sup>6</sup>-benzoic acid]BF<sub>4</sub>}<sub>0.013</sub>.

The nanomagnet-supported catalyst **32** showed a yield and regioselectivity toward the hydroformylation of 4-vinylanisole **31** comparable to its homogeneous counterpart, although it has to be stated that reactions with the unsupported catalyst require only one third of the reaction time (Scheme 9). Nevertheless, the catalyst activity was still extraordinarily high relative to that of catalysts immobilized on conventional supports, for example, polymers,<sup>[37]</sup> and showed



Scheme 9. Hydroformylation of 4-vinylanisole by the nanomagnet-supported catalyst **32**. Ratio of products: **33/34** = 10/90.

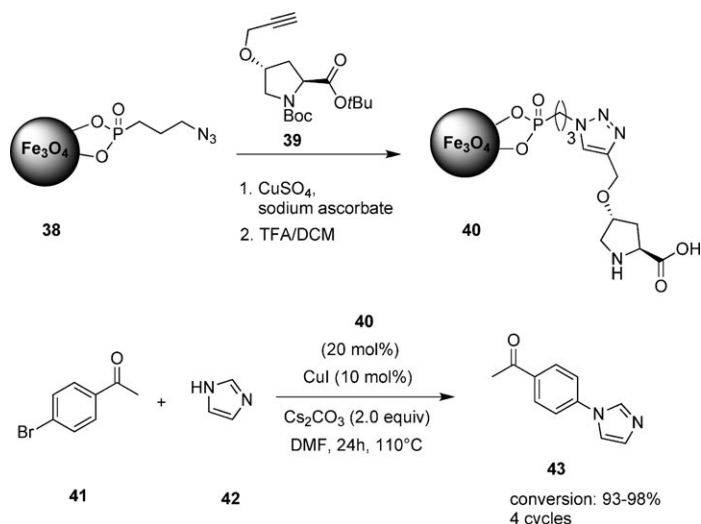
no loss in activity upon recycling by magnetic decantation. Materials like Co-ferrite are a highly magnetic but rather exceptional support. Superparamagnetic materials, such as iron oxide nanoparticles (SPIONs) are far more common since they are intrinsically nonmagnetic (absence of a magnetic field) but readily magnetized in the presence of an additional external magnetic field. Still, low-field magnets are sufficient to recover these particles quantitatively from solution. Furthermore, the lack of magnetic remanence prevents the formation of aggregates in the reaction media. Magnetite ( $\text{Fe}_3\text{O}_4$ ) is not only a widespread representative of such SPION particles but the most common nanomagnetic support par excellence. Phosphonic acid derivatives were successfully used to stabilize magnetite NPs in a number of publications,<sup>[38]</sup> although they were assumed to be less effective in preventing aggregation upon solvent evaporation than oleic acid. Lin et al.<sup>[38a]</sup> used a ruthenium(II) complex with phosphonic acid-substituted BINAP [ $\text{Ru}(\text{BINAP-PO}_3\text{H}_2)(\text{DPEN})\text{Cl}_2$ ] tethered to magnetite nanoparticles which were synthesized either by thermal decomposition or a coprecipitation method (Scheme 10).<sup>[39]</sup>



Scheme 10. Asymmetric hydrogenation of 1-acetonaphthone **35** using a  $\text{Ru}^{\text{II}}$ -BINAP-phosphonic acid catalyst supported on  $\text{Fe}_3\text{O}_4$ -nanoparticles.

Especially magnetite synthesized by the latter route demonstrated outstanding stability, and immobilized catalyst **36** exhibited impressive and simple recycling capabilities via magnetic decantation. A drop in conversion was observed in the 15th cycle of the hydrogenation of 1-acetonaphthone **35** (35%), whereas selectivity remained high (95% *ee*). Catalyst **36** exhibited a saturation magnetization ( $\sigma_s$ ) of  $50 \text{ emu g}^{-1}$ , which is smaller than that of bulk magnetite ( $92 \text{ emu g}^{-1}$ ). Magnetite particles obtained from a similar coprecipitation method served as carriers for a proline ligand that promoted an Ullmann-type coupling between aryl/heteroaryl bromides and nitrogen heterocycles.<sup>[38b]</sup> In contrast to previous protocols, the phosphonic acid derivative was not ligand-functionalized prior to the coating of the particle surface but derivatized in a post-grafting process. To this end, an alkyne moiety was installed on a 4-hydroxyproline

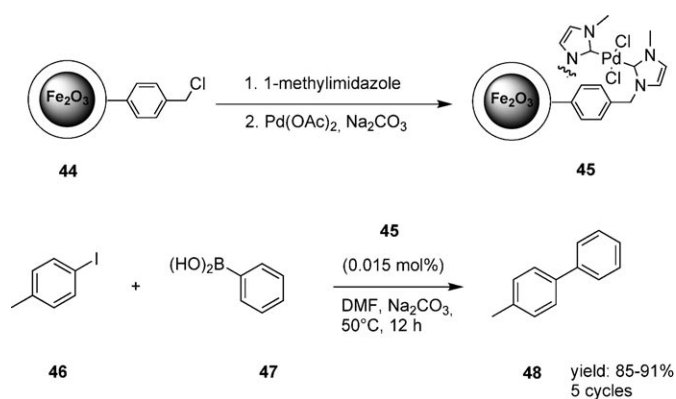
derivative to yield compound **39**, which readily undergoes an azide/alkyne cycloaddition<sup>[40]</sup> reaction in the presence of catalytic amounts of  $\text{Cu}^{\text{I}}$  (Scheme 11).<sup>[41]</sup> Thus, immobilization was achieved by reaction of **39** with simple 3-azidopropylphosphonic acid stabilized magnetite clusters **40** followed by deprotection.



Scheme 11. Synthesis of magnetite supported proline (top) and Ullmann-type coupling reaction of *p*-bromoacetophenone **41** with imidazole **42** promoted by **40** (bottom).

The as-prepared magnetite@proline nanocomposite **40** consisted of partially aggregated particles with a diameter between 6 and 20 nm and exhibited good catalyst loading ( $2.0 \text{ mmol g}^{-1}$ ). The nanomagnets could be reused up to four times without any significant loss of activity. Since phosphonic acids as well as oleate-capped iron oxide nanoparticles sometimes suffer from aggregation due to insufficient stabilization of the discrete clusters, effort was put into the design of additional mantle structures. Gao and co-workers<sup>[42a]</sup> used oleate-protected  $\gamma\text{-Fe}_2\text{O}_3$  nanocrystals and coated them with a thin (2 nm) film of crosslinked polystyrene by using an emulsion-polymerization approach.<sup>[43]</sup> Other strategies were reported as well, such as encapsulation of magnetic beads in a self-assembling Cu-bipyridine chelate and its utilization as oxidation catalyst.<sup>[44]</sup> However, 1,4-vinylbenzene chloride was copolymerized to allow the immobilization of 1-methylimidazole, which formed N-heterocyclic carbenes (NHC) upon deprotonation. NHCs were chosen as ligands for chelating Pd because of the impressive complex stability of these compounds (Scheme 11).<sup>[45]</sup> The catalytic power of this system was tested in a range of Suzuki cross-coupling reactions of aryl halides with arylboronic acids. In this context, SPION-supported Pd catalyst **45** showed better catalytic activity than chloromethyl polystyrene resin-supported counterparts reported in the literature.<sup>[46]</sup> Finally, maghemite-supported Pd catalyst **45** was subjected to five iterative reactions between *p*-iodotoluene **46** and phenylboronic acid **47** to demonstrate its recyclability (Scheme 12).

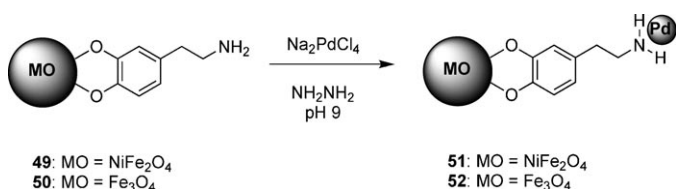




Scheme 12. Suzuki cross-coupling of 4-iodotoluene (**46**) with phenylboronic acid (**47**) catalyzed by PS-coated SPION@NHC-Pd **45**.

### Dopamine-Capped Ferrite Nanoparticles

Enediol ligands such as catechols are known to have a high affinity for under-coordinated surface sites of metal oxide nanoparticles.<sup>[47]</sup> Therefore, dopamine has attracted some attention since it features an additional amine moiety that allows either immobilization of metal centers or further covalent modification.<sup>[48]</sup> Manorama and co-workers<sup>[49]</sup> reported several examples of palladium(0)-doped ferrite particles (NiFe<sub>2</sub>O<sub>4</sub> and Fe<sub>3</sub>O<sub>4</sub>). The dopamine (DOPA) layer was formed by refluxing or sonicating the ferrites together with the catecholamine in water. Once a Pd species was anchored on the nanomagnets (Scheme 13), the saturation magnetiza-

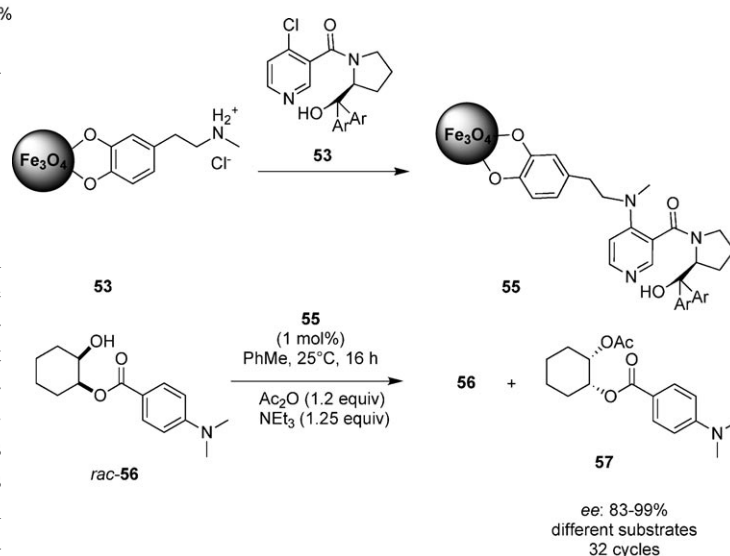


Scheme 13. Synthesis of ferrite-dopamine nanocomposite doped with Pd<sup>0</sup>.

tion of the spinel ferrite and magnetite supported Pd-DOPA **51** and **52**, respectively, dropped significantly. For a series of hydrogenation reactions with catalysts **51** and **52** including aromatic nitro and azide compounds to their respective amine derivatives, the activities observed exceeded those of previous studies.<sup>[50]</sup> The activity of **52** was somewhat inferior due to a lower palladium loading on the surface. Even after 10 cycles, no deterioration in catalytic efficacy of both catalysts occurred.<sup>[49c]</sup> In addition, the spinel-supported catalyst **51** was applied for Suzuki and Heck coupling reactions with several aromatic halide derivatives.

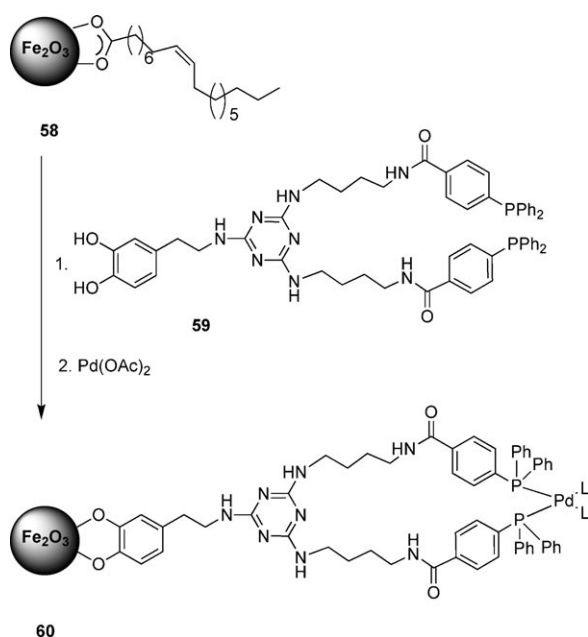
Varma et al. described the synthesis of nickel-, ruthenium-, and palladium-doped ferrite nanoparticles for hydrogenation and oxidation reactions following a similar route.<sup>[51]</sup> The stability of this relatively simple tagging method for metal oxide nanoparticles was impressively demonstrated in

an extensive study by Gun'ko, Connon and co-workers.<sup>[52]</sup> A proline-derived chiral 4-dimethylaminopyridine (DMAP) was fused with DOPA-capped magnetite nanoparticles, thus resulting in catalyst **55**, which exhibited unprecedented recyclability. It was reused 32 times for the asymmetric acylation of different *sec*-alcohol substrates, mostly monoprotected vicinal diols, retaining high activity and selectivity profiles (Scheme 14). Furthermore, TEM images of the nanocatalyst did not reveal any morphological alterations that could be attributed to particle degradation.



Scheme 14. Preparation of a chiral DMAP/DOPA@magnetite catalyst for the asymmetric acylation of secondary alcohols.

Catecholamines can additionally act as cornerstones for more complex molecular architecture on iron oxide nanoparticles, which allows the tuning of solubility and enables complex formation. Gao et al.<sup>[53]</sup> reported on maghemite ( $\gamma$ -Fe<sub>2</sub>O<sub>3</sub>) NPs protected with a shell of Simanek-type<sup>[54]</sup> (melamine) dendrons footing on a dopamine linker. Different generations of Simanek-type building blocks were modified with dopamine, which enabled these dendritic branches to undergo a place-exchange reaction with the oleate surfactants.<sup>[55]</sup> Up to three dendron generations were anchored on a maghemite core in this way. Triphenylphosphine moieties on the termini of generation-one dendrons could be used to allow the formation of Pd complexes on the surface of the dendrimer-like core-shell structure (Scheme 15). The as-prepared dendron-coated iron oxide NPs were able to promote Suzuki cross-coupling reactions of several aryl halides with phenylboronic acid **47** at a catalyst concentration of 5 mol % under conditions comparable to those given in Scheme 12. In addition, **60** was found to maintain its activity upon recycling. Very recently, another highly active metalodendron based on polymer-coated maghemite was reported.<sup>[56]</sup> It was likewise functionalized with a diphosphinopalladium complex for Suzuki cross-coupling reactions but allowed recycling more than 25 times with almost no loss in reactivity.



Scheme 15. Representative diagram for the synthesis of  $\gamma\text{-Fe}_2\text{O}_3$  nanoparticles protected by first-generation Simanek-type dendrons possessing Pd–triphenylphosphine moieties.

### Silica-Coated Ferrite Nanoparticles

Apart from enediol ligands, silanes are frequently used to coat ferrites.<sup>[57]</sup> The deposition and adhesion of silica can be achieved by the hydrolysis of a sol–gel precursor to give shells with a thickness between 2 and 100 nm. Because of the strong affinity of iron oxide surfaces toward silica, no primer is required. An advantage of the silica coating is that its surface is terminated by silanol groups, which can react with various coupling agents to covalently attach linkers, ligands, metals, or complexes. As with catechols, silanes are able to replace simple carboxylate ligands, hence, Gao et al. used an oleate-stabilized precursor for the synthesis of  $\text{Fe}_2\text{O}_3@\text{SiO}_2$  (Scheme 16, top).<sup>[42b]</sup> Nanocomposites of this kind were extensively used for palladium-catalyzed cross-coupling reactions.<sup>[58]</sup> In addition, an interesting application for the immobilized NHC–Pd catalyst **61** was presented by Gao et al., that is, taking advantage of the ability of the nanomagnet **61** to enter the polystyrene backbone (1% divinylbenzene-crosslinked polystyrene) of a solid-phase supported arylhalogenide **62**.<sup>[42c]</sup> The two supports **61** and **62** may be considered orthogonal due to the different separation procedure. Together with phenylboronic acid **47** in the solvent phase, this system furnished a three-phase Suzuki cross-coupling reaction (Scheme 9, bottom). The Pd catalyst was recovered from the reaction mixture with the aid of an external magnet. Subsequently, filtration removed the excess of dissolved borate reagent from the resin/product. Finally, the cross-coupling product **63** was cleaved from the polymer by basic hydrolysis.

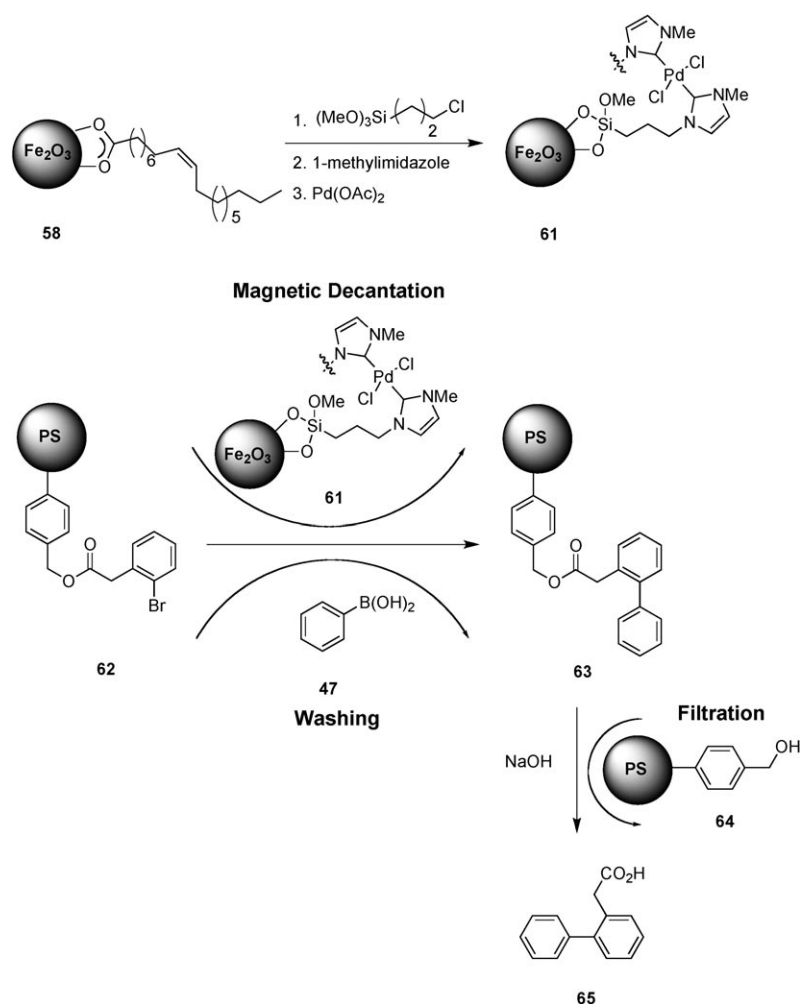
The ability of nanoparticles to penetrate the pores of certain polymers has inspired their use in polymer synthesis. In

general, the purification of polymers can be challenging already with a homogeneous catalyst since separation through copious washing is tedious. Therefore, a catalyst support being small enough to pass the polymer coils is a prerequisite for efficient recycling. Moreover, a support that can be attracted by an external magnetic field might be apt to reduce the amount of solvent necessary for complete removal of catalyst. Following this line of argument, Shen and co-workers<sup>[59]</sup> developed a magnetite-anchored atom transfer radical polymerization (ATRP)<sup>[60]</sup> catalyst with an average particle diameter of 25 nm (Scheme 17).

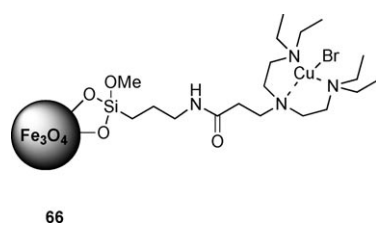
Catalyst **66** mediated the polymerization of methyl methacrylate (MMA) in a manner similar to homogeneous catalysts, thus being in contrast to catalysts immobilized on comparatively “large” particles, whose resulting polymers had uncontrolled molecular weights and high polydispersity. After recycling, **66** showed slightly diminished activity, which decreased further after another cycle. The authors reasoned that oxidation of copper(I) might be responsible for this effect. To overcome this problem, in situ catalyst regeneration methods were developed, for example, triethylamine was used to reduce any  $\text{Cu}^{\text{II}}$ .<sup>[59b]</sup> Indeed, recycled catalyst **66** regained high activity and excellent control over polymerization after in situ regeneration. Admittedly, the formation of well-defined transition-metal complexes on the surface of the shells is tedious and not necessarily suggested for every reaction. Early representatives of “magnetic silica” were doped with palladium nanoclusters by using amine- or thiol-affinity ligands. In fact, Schüth and co-workers<sup>[61]</sup> were the first to disclose the perspectives of magnetically separable mesoporous silica; however, Ying et al.<sup>[62]</sup> reported  $\text{SiO}_2$ -coated maghemite nanoparticles that served as a catalyst support. In a straightforward synthesis, maghemite@silica was refluxed with either (3-mercaptopropyl)trimethoxysilane (MPS) or *N*-(2-aminoethyl)-3-aminopropyltrimethoxysilane (AAPS) in toluene for 30 h to yield **67** and **68** respectively (Scheme 18).

Next, palladium nanoclusters were deposited on the surface of the affinity-ligand-functionalized  $\text{Fe}_2\text{O}_3@\text{SiO}_2$  particles under microwave irradiation.  $\text{Fe}_2\text{O}_3@\text{SiO}_2@\text{Pd}$  nanocomposites of **67** and **68** were examined as catalysts for the hydrogenation of nitrobenzene to aniline. Both gave 99% conversion over five consecutive runs. Their conversions then decreased gradually in subsequent runs to 87% and 76%, respectively, at run 14. The conversion after multiple catalyst recycling was reduced through agglomeration of the Pd clusters, especially in the case of  $\text{Fe}_2\text{O}_3@\text{SiO}_2\text{-SH}@\text{Pd}$ . TEM images taken before and after 14 runs confirmed this hypothesis (Figure 3).

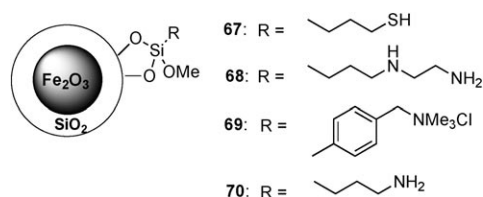
The catalytic activity is known to be related with Pd cluster size and shape.<sup>[63]</sup> The authors concluded that AAPS might serve as a stronger affinity ligand than MPS, thus suppressing the aggregation of palladium. Kirschning et al. used a nanocomposite prepared by the reductive precipitation of tetrachloropalladate salts bound on magnetic NPs **69** as a packed bed inside a flow reactor.<sup>[64]</sup> Moreover, they disclosed inductive heating as a simple and efficient alternative



Scheme 16. Synthesis of a NHC–Pd complex tagged on silica-coated maghemite-nanoparticles by a place-exchange reaction with oleate-stabilized iron oxide nanocrystals (top) and representation of its utilization in a magnetic nanoparticle facilitated solid-phase Suzuki cross-coupling reaction (bottom).



Scheme 17. A tetraethyldiethylenetriaminocopper(I) complex for the polymerization of methyl methacrylate (MMA) supported on magnetite via a silane agent.



Scheme 18. Different silica-coated ferrite nanoparticles with thiol and amine tags.

to microwave irradiation for this kind of material in a flow-through system. Several Suzuki–Miyaura and Heck reactions were performed with that technique, thus giving proof that the catalyst remained active for at least three consecutive runs. As a minor drawback, moderate palladium leaching was observed (up to 100 ppm), albeit this is still at a reasonable level taking into account the forcing reaction conditions.

Similar to catecholamine-stabilized iron oxide nanocrystals, silica-coated cores can be dendronized to make them more stable and soluble in organic solvents. Just like on dendronized  $\text{Fe}_2\text{O}_3\text{@DOPA}$  **60**, phosphonated moieties can be introduced to chelate transition metals. To this end, Post and co-workers<sup>[65]</sup> grew up to three generations of a polyaminoamido (PMAM) dendron on silanized iron oxide. Interestingly, without silica coating the growth of dendrons could not be achieved. The dendrons were phosphonated by reaction of the terminal amino groups with diphenylphosphinmethanol prepared in situ from diphenylphosphine and paraformal-

dehyde. Although the amount of amino groups increased with the growth of the dendrons to higher generations, the phosphorus content remained almost the same because of incomplete phosphination due to steric hindrance. The phosphonated dendrons were subsequently complexed with  $[\{\text{Rh}(\text{cod})\text{Cl}_2\}]$  (Scheme 19).

The resulting complex **72** was tested in hydroformylation reactions using a 1:1 mixture of carbon monoxide and hydrogen pressurized to 1000 psi. The selectivity toward the branched product was high and catalysts were more reactive and selective when compared with those used in previous studies.<sup>[66]</sup> G(1) dendrimer based catalyst **72** was able to maintain its activity for at least five iterative runs. In contrast to previous studies,<sup>[66c]</sup> moving to higher generations did not involve loss of activity and selectivity. The present catalytic systems, grafted on up to three dendron generations, retained their efficacy.

Silica-coated magnetic nanoparticles are certainly among the most versatile scaffolds, since the metal oxide core is shielded effectively from its surrounding environment.

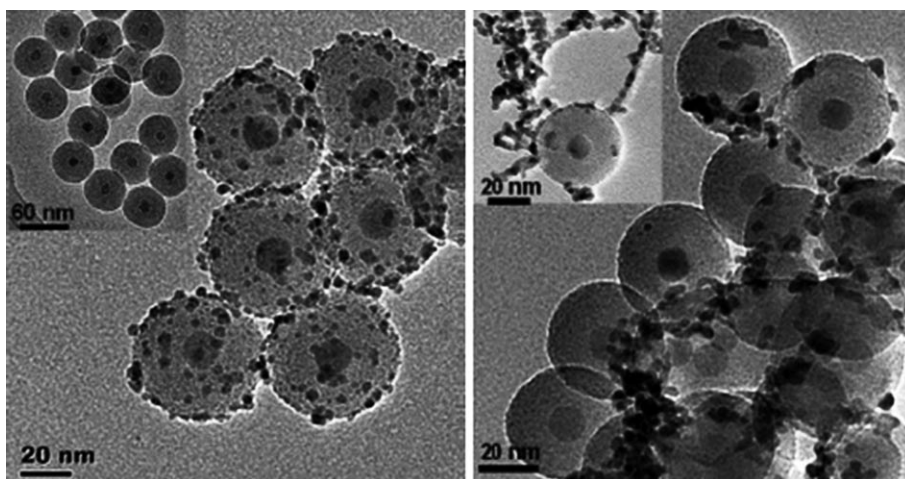
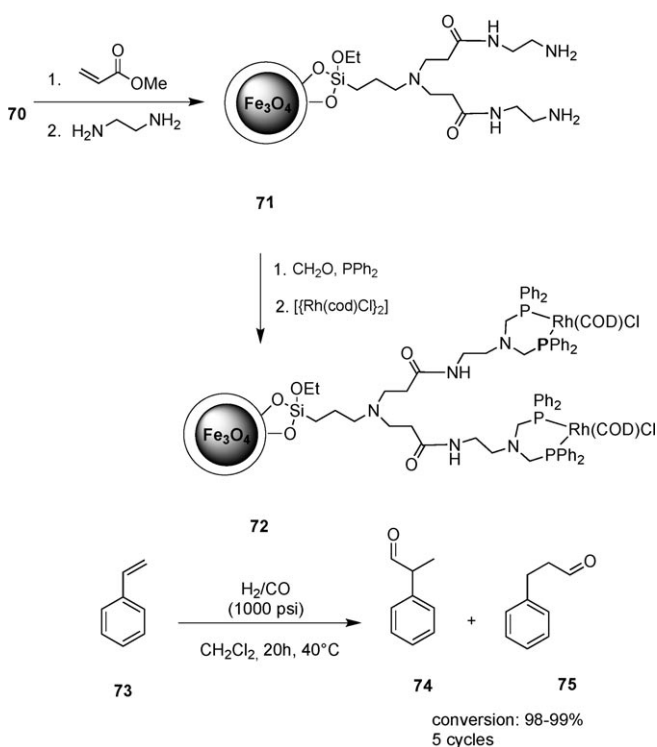


Figure 3. TEM images of  $\text{Fe}_2\text{O}_3@\text{SiO}_2\text{-SH@Pd}$  taken before (left) the first and after the 14th run (right) of nitrobenzene hydrogenation. The inset in the right picture shows that the Pd nanoclusters interconnected and some of them became detached from the support. Reprinted with kind permission.<sup>[62]</sup>

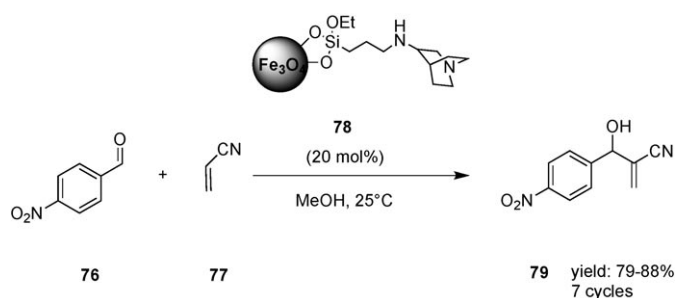


Scheme 19. Procedure for the dendronization, phosphination and complexation with  $[\text{Rh}(\text{cod})\text{Cl}]_2$  of silica-coated iron oxide nanoparticles for the hydroformylation of styrene.

Hence, this support was recently used for a number of organocatalysts.<sup>[67]</sup> Cannon et al. were the first to report an organocatalyst tethered to a  $\text{Fe}_3\text{O}_4@\text{SiO}_2$  nanomagnet.<sup>[68]</sup> They evaluated achiral DMAP as an antecedent of its chiral counterpart (Scheme 14) in the acetylation of 1-phenylethanol by acetic anhydride where it furnished the acetylated product in 14 iterative cycles with excellent conversion in each case.

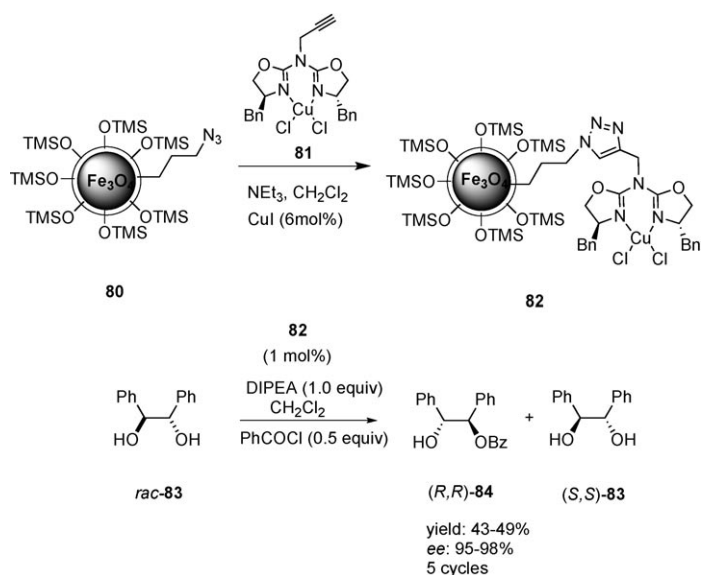
The recovered material was subsequently found to be even active when employed at loadings as low as 0.2 mol%. The reaction scope was further examined by subjecting the recycled catalyst to a range of distinct transformations where it acted as a nucleophilic catalyst. After 30 iterative cycles, it was still able to achieve an almost identical level of conversion (80%) in the acetylation of phenylethanol. At the time, this was an unprecedented level of recyclability, which was excelled only by its chiral successor **56**.<sup>[52]</sup> Shortly after, Cheng et al. published a magnetite@silica-grafted quinuclidine that promoted the Morita–Baylis–Hillman reaction as efficiently as commercial 1,4-diazobicyclo[2.2.2]octane (DABCO) and was more active than a simple silica-bound analogue (Scheme 20).<sup>[69]</sup> Moreover, **78** could be reused basically without any loss of activity.

More recently, Cheng et al. published a magnetite@silica-grafted quinuclidine that promoted the Morita–Baylis–Hillman reaction as efficiently as commercial 1,4-diazobicyclo[2.2.2]octane (DABCO) and was more active than a simple silica-bound analogue (Scheme 20).<sup>[69]</sup> Moreover, **78** could be reused basically without any loss of activity.



Scheme 20. Magnetically separable quinuclidine **78** for the Morita–Baylis–Hillman reaction.

Examples for chiral transition-metal complexes on silica-coated nanoparticles are rather rare. Li et al.<sup>[70]</sup> entrapped  $\gamma\text{-Fe}_2\text{O}_3$  in a siliceous mesocellular foam that was decorated with a chiral diamine ligand for the ruthenium-catalyzed transfer hydrogenation of aldehydes and ketones. Although this concept is not based on core–shell assemblies, it ought to be mentioned in this regard since the immobilized Ru–TsDPEN (*N*-(*p*-toluenesulfonyl)-1,2-diphenylethylenediamine) complex furnished high yields and *ee* values in at least nine runs. The first example of an enantioselective metal complex grafted on discrete SPION particles was published by Reiser et al.<sup>[71]</sup> An azabis(oxazoline)copper complex was “clicked”<sup>[41]</sup> on azide-functionalized  $\text{Fe}_3\text{O}_4$  coated with amorphous silica (Scheme 21). The preparation of the azide-terminated NPs was achieved in a simple one-pot reaction. The nanocatalyst **82** outperformed its analogues on soluble (MeOPEG) and insoluble (polystyrene) polymeric



Scheme 21. Copper(I)-catalyzed azide/alkyne cycloaddition reaction of azabis(oxazoline)copper complex **81** and azide-functionalized magnetite@silica nanoparticles (top) and application of the resulting catalyst **82** in the kinetic resolution of racemic 1,2-diol (**83**).

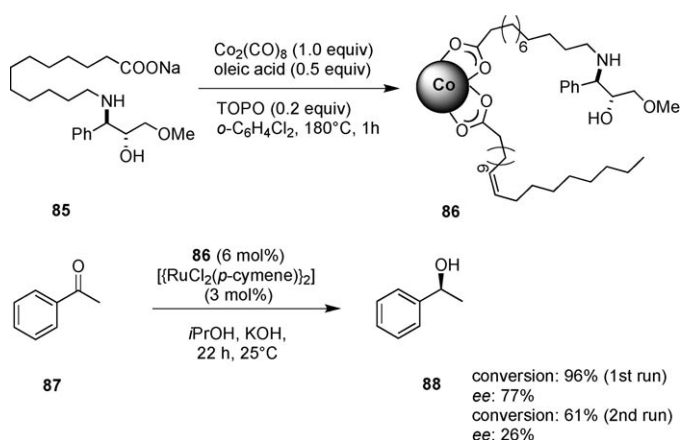
supports, respectively, in the kinetic resolution of racemic 1,2-diol via asymmetric benzylation in terms of activity and selectivity (Scheme 20).

A prerequisite for these high levels of induced enantioselectivity was the TMS capping of residual hydroxyl groups on the silica surface to avoid interactions of the silanol moieties with copper. Copper salts on the silica surface lack a stereodiscriminating environment. Hence, such catalytic centers would result in racemic products and therefore diminish the overall *ee* value. Spatial interactions between the ligands are potentially detrimental as well, thus, the loading and therefore catalyst density on the surface was kept low (0.1–0.3  $\text{mmol g}^{-1}$ ).

## Carbon-Coated Metal Nanoparticles

Apart from the magnetic metal oxides, pure metals such as Fe, Co, and Ni and their metal alloys were used in various fields requiring magnetic materials.<sup>[72]</sup> The saturation magnetization of these ferromagnets exceeds the values obtained with ferrites, for example, magnetite ( $M_{\text{S,bulk}} \leq 92 \text{ emu g}^{-1}$ ), by far (Co, Fe:  $M_{\text{S,bulk}} \leq 220 \text{ emu g}^{-1}$ ; CoFe, CoNiFe: ( $M_{\text{S,bulk}} \leq 245 \text{ emu g}^{-1}$ ). On the other hand, nanoparticles of pure metals are highly sensitive to air and may even be pyrophoric, whereas oxidation of the aforementioned magnetite particles to maghemite is less problematic. Thus, a suitable coating for metal NPs has to take various factors into consideration. Nevertheless, cobalt metal nano-clusters are also known to be efficiently stabilized by oleic acid.<sup>[73]</sup> A recent example shows that even this rather penetrable carboxylate layer can enable Co-NPs to act as recyclable carriers. Pericàs et al. reported on nanosized  $\epsilon$ -cobalt,

stabilized with oleic acid and long chained carboxylic acids functionalized with chiral  $\beta$ -amino alcohols (Scheme 22).<sup>[74]</sup> The presence of oleic acid during this synthesis is crucial

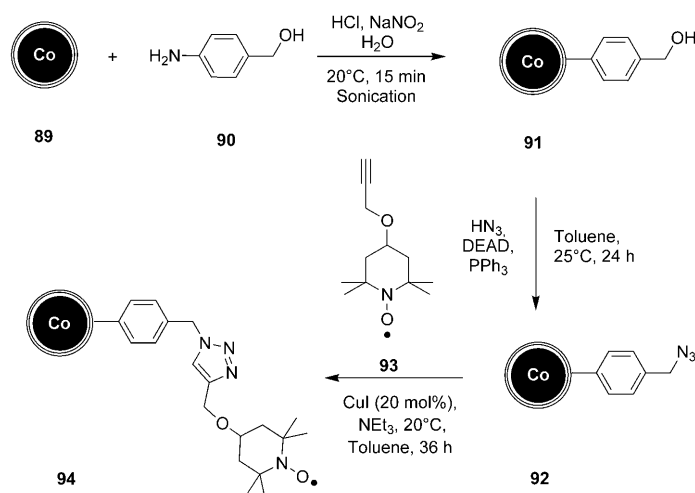


Scheme 22. Synthesis of oleic acid capped cobalt nanoparticles functionalized with chiral amino alcohol for the Ru-catalyzed transfer hydrogenation of acetophenone **87**.

since no stable nanomaterial can be obtained without it. Particle size and loading strongly depend on the nature of the amino alcohol. For example, amino alcohol derivative **85** furnished a loading of  $1.4 \text{ mmol g}^{-1}$  and a mean cluster diameter of 13 nm. It served as a magnetically recyclable ligand for the ruthenium-catalyzed transfer hydrogenation of ketones, for example, acetophenone **87** (Scheme 22). It was found that activity and selectivity of the grafted complex were reasonably higher than values obtained with the free amino alcohol. The authors reasoned that the concave active site formed on the surface of the nanostructure induced this beneficial effect.

However, the recovered catalyst was limited in terms of yield and selectivity when applied in a second run, even if fresh  $[\{\text{RuCl}_2(p\text{-cymene})\}_2]$  was added. Leaching of functionalized carboxylates from the nanoparticles might have contributed to this explicit drop. Moreover, without the addition of ruthenium, virtually no conversion was observed. Reduction of the ruthenium complex by metallic cobalt was thought responsible for this effect. This pioneering work on pure metallic core materials as catalyst support demonstrated once more the need for a suitable shell material to protect the labile metal cores. Silica coatings are sufficiently stable as long as harsh basic conditions are avoided and have therefore gained a predominant position for the passivation of iron oxide nanoparticles, as pointed out in the previous chapter. However, a primer has to be used to make the surface of metal nanoparticles glasslike (“vitro-philic”)<sup>[75]</sup> to create an additional barrier for oxygen and other species that could diffuse through pores in the silica. Carbon layers provide definitely the highest level of chemical and thermal stability over all aforementioned organic and inorganic compounds.<sup>[76]</sup> Despite this benefit, the formation of carbon-coated metal particles was challenging and

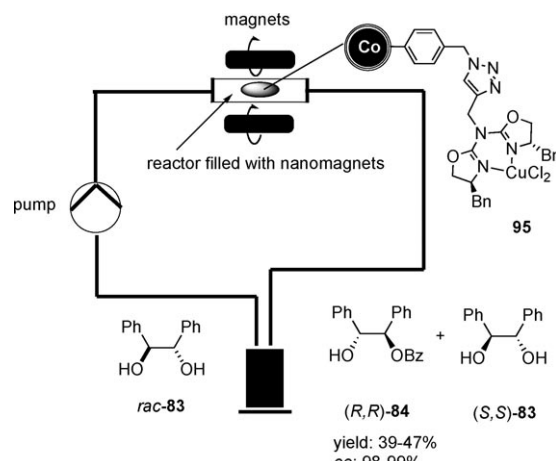
possible only in small-scale operations ( $< 1 \text{ g h}^{-1}$ ) via arc discharge techniques,<sup>[77]</sup> chemical vapor depositions,<sup>[78]</sup> and pyrolysis of metal complexes.<sup>[79]</sup> Recently, Grass et al.<sup>[80]</sup> reported on different metal nanoparticles on which a graphene layer (1 nm) was deposited by reducing flame-spray pyrolysis.<sup>[81]</sup> This procedure gave rise to substantial amounts of metal nanoparticles ( $> 30 \text{ g h}^{-1}$ ), which is of course a prerequisite for their application as catalyst support. Moreover, the thermal and chemical stability of this material, even under harsh acidic conditions, was remarkable.<sup>[82]</sup> The graphene layer can be covalently functionalized and offers a versatile and reliable attachment to ligand backbones via C–C bonding.<sup>[80a,83]</sup> Stark and Reiser anchored the stable nitroxyl radical 2,2,6,6-tetramethylpiperidine-1-oxyl (TEMPO), an organocatalyst for the chemoselective oxidation of primary and secondary alcohols, on carbon-coated cobalt nanoparticles by using a “click” protocol.<sup>[84]</sup> To this end, the Co/C nanopowder was azide-tagged by way of covalently bound aryl compounds, which were formed on the graphene surface by the decomposition of diazonium precursor **90** (Scheme 23).



Scheme 23. Grafting of the diazonium salt of 4-aminobenzyl alcohol (**90**) onto carbon-coated cobalt particles and subsequent “click” reaction between azide-modified particles **92** and propargylated TEMPO **93**.

This covalent attachment through a triazole linker is known to persist over a wide pH range. Co/C-TEMPO **94** promoted the oxidation of several benzylic and aliphatic alcohols into the corresponding aldehydes in 14 consecutive runs without significant loss of activity. In addition, the recovered material did not show any morphological alterations after several cycles in TEM studies. No hitherto existing nanoparticle support had demonstrated such performance under the harsh oxidative conditions (alkaline chlorine bleach) of TEMPO-mediated oxidations until then, although examples of NP-anchored TEMPO were reported.<sup>[85]</sup> The stability and inertness of the graphene layer is one argument for metal/carbon assemblies. Moreover, the magnetic properties of such metallic nanoparticles are quite pronounced.

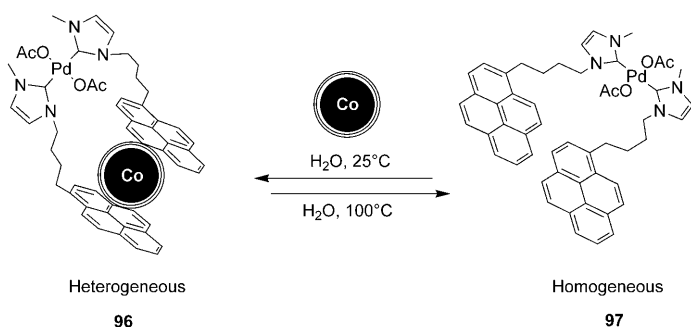
This qualifies them for applications restricted to highly magnetic materials, for which SPION particles might not be suited in every case. Reiser and Stark tested azabis(oxazoline)copper complexes on magnetite@silica and Co/C-NPs respectively in a continuous-flow reactor as a conceptual alternative to fixed-bed reactors.<sup>[86]</sup> Magnetic fluidization of the nanoparticle-supported catalyst in the microreactor was expected to make the application of membranes for nanofiltration dispensable. In theory, clogging of the membrane, which would inevitably provoke a flow-collapse, could be avoided and fluid dynamics would be improved. Therefore, the free-floating nanocatalyst had to be retained magnetically in the reactor. When Fe<sub>3</sub>O<sub>4</sub>@SiO<sub>2</sub>-tagged catalyst **82** was employed, excessive leaching occurred immediately even at moderate flow rates (0.2 mL min<sup>-1</sup>). Thus, SPION particles with their comparatively low saturation magnetization (20 emu g<sup>-1</sup>) appeared ineligible for this setup. In contrast, the carbon-coated cobalt particles (158 emu g<sup>-1</sup>) were retained showing only negligible nanoparticle leaching ( $< 1\%$  after 60 h). The resulting material was able to resolve several batches of racemic 1,2-diol **83** fed into the closed circuit reactor (Scheme 24). Although selectivities were excellent, reaction times were significantly prolonged, most probably due to the inevitable dilution of reactants.



Scheme 24. Representation of a continuous-flow reactor for the asymmetric monobenzylation of racemic diol **83** with magnetic fluidization/containment of catalytic nanomagnets inside the microreactor.

Not only the properties of the core material but also the chemical and physical properties of the shell enable novel strategies in catalyst separation. Carbon surfaces feature the possibility of noncovalent functionalization through  $\pi$ – $\pi$  stacking interactions with highly aromatic compounds.<sup>[87]</sup> The attraction to the graphene layer is sufficiently strong to prevent any unintended dissociation of the immobilized compounds in polar solvents, thus offering a very concise route for the grafting of catalysts. On the contrary, dissociation of a tethered complex can even be intended when a catch–release strategy is desired. Stark, Reiser, and co-workers<sup>[88]</sup> reported on a palladium complex, noncovalently at-

tached to Co/C-NPs via pyrene tags, for the hydroxycarbonylation of aryl halides in water. In this case, the desorption of the aromatic anchors was thermally triggered to allow the catalyst to become homogeneous during the course of the reaction at 100°C. Once the reaction was finished and the solution cooled to ambient temperature, the pyrene moieties could be re-absorbed on the carbon surface (Scheme 25).



Scheme 25. A palladium(NHC)-complex noncovalently attached to Co/C nanoparticles via pyrene tags for a thermally triggered catch-release system.

The absorbed complex was amenable to magnetic decantation and therefore recycled 16 times. Catalyst leaching into the product phase, a potential drawback of this “boomerang” catalyst, proved to be negligible (0.7 ppm).

## Summary and Outlook

This Review highlights recent achievements in the field of particle-supported nanocatalysis, that is, by immobilization of catalysts on the surface of globular core-shell assemblies, and the immanent potential in this emerging area. In theory, catalysts anchored on the surface of highly dispersible and quantitatively recyclable nanoparticles promise reaction rates and selectivities that are usually restricted to their homogeneous counterparts. Cooperative catalysis and interphase effects allowed the grafted complexes to perform even better than their soluble analogues in particular cases.<sup>[20,29,30]</sup> However, mass transport limitations and difficulties to control the degree of confinement along with clustering of for example, palladium catalysts on the surface are usually detrimental to rates.<sup>[63]</sup> The choice of the core material and coating can influence the performance of the grafted catalyst dramatically, for example, a BINOL complex tethered to AuMPCs might be highly active,<sup>[21]</sup> whereas the same compound lacks reactivity on maghemite NPs.<sup>[5]</sup> Although factors such as spatial interference of the active sites on the periphery and spacer length demand fine-tuning, the chemical and physical properties of the structural bulk material are crucial.<sup>[80]</sup> Any detrimental interaction of the core material with catalyst has to be prevented by the choice of a suitable mantle structure.<sup>[74]</sup> Moreover, reaction rates depend on the efficient dispersion of the nanoparticles,

which is usually more feasible for smaller particles. However, comparatively little space was dedicated to the itemization of the mean particle diameter of the discrete core-shell structures in the previous chapters, since a wrong impression of the actual dimension of the nanocomposites would be given as long as the degree of polydispersity and particle aggregation are not considered. Counterintuitively, especially very small nanoparticles might result in comparatively large aggregates.<sup>[89]</sup> All nanosized assemblies suffer from this intrinsic tendency to agglomerate, thus reducing the energy associated with the high surface area/volume-ratio. Consequently, materials that are denoted “nano” might not exhibit a relevant population of matter in a dimension that justifies this tag. The formation of aggregates might be detrimental for reaction rates, but does not necessarily affect the lifetime of the discrete nanoparticles since agglomeration is reversible if stable coatings are used rather than surfactants.

Magnetic materials usually offer opportunities that largely outnumber the potential disadvantages. Magnetically driven separations make the recovery of catalysts in a liquid-phase reaction more feasible than techniques relying on crossflow filtration and centrifugation. Naturally, the affinity to coalescence is enhanced in ferromagnetic particles, thus making the formation of dispersions and the coating process itself more challenging. Even though such problems are far less tantalizing if superparamagnetic iron oxide nanoparticles (SPION) are handled, pure metals and alloys are highly attractive since they exhibit superior magnetic behavior, that is, saturation magnetization. Ultimately, well-defined superparamagnetic metal nanoparticles accessible in large scale and low cost would be the destination. For all practical purposes, this is an almost insurmountable obstacle since already a small percentage of the produced material being ferromagnetic (in plain terms: too large) would induce overall remanent magnetism. In any case, the coating should be able to exclude oxygen, a problem that was effectively addressed with shells derived from inorganic components, including silica,<sup>[90]</sup> precious metals, such as Ag and Au,<sup>[91]</sup> and especially carbon<sup>[92]</sup> rather than organic compounds (e.g. surfactants, polymers).<sup>[93]</sup> Carbon-coated metal particles bear great potential since they furnish a material that is nearly indestructible, characterized by a vast resistibility to environmental impairment, for example, heat or acid.<sup>[80,82]</sup> In addition, strategies for their covalent functionalization comply with that inertness. The issue of a coating that is able to provide the metal cores with physical and chemical stability at least on a par with polymer<sup>[94]</sup> and dendrimer<sup>[95]</sup> supports, was rarely discussed. This is understandable in part because often enough metal leaching from organometallic complexes is the limiting factor for catalyst recycling. However, certain complexes and organocatalysts put the resistibility of the scaffold to the test and call for supports that are stable in an expanded pH range.

In summary, huge effort was placed in the development of systems that minimize the influence of the support on the catalyst and are capable of efficient recycling at the same time. Catch-release systems, as depicted at the very end of



the previous chapter (Scheme 25), might be a promising tool en route to catalysts that are actually homogeneous and not only “semi-heterogeneous”. Next to classical metal-mediated and organocatalytic reactions, nanoparticle-bound enzymatic and biomimetic catalysts (e.g. “nanozymes”) are a fascinating emerging area that was omitted in this article.<sup>[96]</sup> Overall, the field of nanocatalysis is expanding dramatically, most novel nanosized materials and applications are yet to be explored.

## Acknowledgements

Financial support by the ETH Zurich, the IDK NanoCat (Elitenetzwerk Bayern), and the Swiss National Science Foundation is kindly acknowledged.

- [1] J. Grunes, J. Zhu, G. A. Somorjai, *Chem. Commun.* **2003**, 2257.
- [2] Reviews: a) G. Schmid, *Chem. Rev.* **1992**, 92, 1709; b) L. N. Lewis, *Chem. Rev.* **1993**, 93, 2693; c) R. M. Crooks, M. Zhao, L. Sun, V. Chechik, L. K. Yeung, *Acc. Chem. Res.* **2001**, 34, 181; d) J. Schulz, A. Roucoux, H. Patin, *Chem. Rev.* **2002**, 102, 3757; e) M. Fernandez-Garcia, A. Martinez-Arias, J. C. Hanson, J. A. Rodriguez, *Chem. Rev.* **2004**, 104, 4063; f) D. Astruc, F. Lu, J. R. Aranzas, *Angew. Chem.* **2005**, 117, 8062; *ngew. Chem. Int. Ed.* **2005**, 44, 7852; g) A.-H. Lu, E. L. Salabas, F. Schueth, *Angew. Chem.* **2007**, 119, 1242; *Angew. Chem. Int. Ed.* **2007**, 46, 1222; h) S. Roy, M. A. Pericàs, *Org. Biomol. Chem.* **2009**, 7, 2669; i) M. R. Buchmeiser, *Chem. Rev.* **2009**, 109, 303; j) Z. Wang, G. Chen, K. Ding, *Chem. Rev.* **2009**, 109, 322; k) A. F. Trindade, P. M. P. Gois, C. A. M. Alfonso, *Chem. Rev.* **2009**, 109, 418.
- [3] J. M. Thomas, W. J. Thomas, *Principles and Practice of Heterogeneous Catalysis*, VCH, Weinheim, **1997**.
- [4] See, for example: a) M. Studer, H.-U. Blaser, C. Exner, *Adv. Synth. Catal.* **2003**, 345, 45; b) S. Jansat, M. Gómez, K. Philippot, G. Müller, E. Guieu, C. Claver, S. Castillón, B. Chaudret, *J. Am. Chem. Soc.* **2004**, 126, 1592; c) K. H. Park, Y. K. Chung, *Adv. Synth. Catal.* **2005**, 347, 854; d) S. Jansat, D. Picurelli, K. Pelzer, K. Philippot, M. Gómez, G. Müller, P. Lecante, B. Chaudret, *New J. Chem.* **2006**, 30, 115.
- [5] a) J. Fan, Y. Gao, *J. Exp. Nanosci.* **2006**, 1, 457; b) J. D. E. T. Wilton-Ely, *Dalton Trans.* **2008**, 25.
- [6] Reviews: a) C. A. McNamara, M. J. Dixon, M. Bradley, *Chem. Rev.* **2002**, 102, 3275; b) D. E. Bergbreiter, *Chem. Rev.* **2002**, 102, 3345; c) R. van Heerbeek, P. C. J. Kamer, P. W. N. M. van Leeuwen, J. N. H. Reek, *Chem. Rev.* **2002**, 102, 3717; d) I. F. J. Vankelecom, *Chem. Rev.* **2002**, 102, 3779.
- [7] A. R. Vaino, K. D. Janda, *J. Comb. Chem.* **2000**, 2, 579.
- [8] A. Thayer, *Chem. Eng. News* **2005**, 83, 55.
- [9] a) Z. Luo, Q. Zhang, Y. Oderaotoshi, D. P. Curran, *Science* **2001**, 291, 1766; b) L. V. Dinh, J. A. Gladysz, *Chem. Commun.* **2004**, 998.
- [10] J. C. Love, L. A. Estroff, J. K. Kriebel, R. G. Nuzzo, G. M. Whitesides, *Chem. Rev.* **2005**, 105, 1103.
- [11] M.-C. Daniel, D. Astruc, *Chem. Rev.* **2004**, 104, 293.
- [12] D. L. Huber, *Small* **2005**, 1, 482.
- [13] Z. P. Xu, Q. H. Zeng, G. Q. Lu, A. B. Yu, *Chem. Eng. Sci.* **2006**, 61, 1027.
- [14] a) S. Benderbous, C. Corot, P. Jacobs, B. Bonnemain, *Acta Radiol.* **1996**, 3, 292; b) Q. A. Pankhurst, *BT Technology J.* **2006**, 24, 33; c) P. Tartaj, M. P. Morales, S. Veintemillas-Verdaguer, T. Gonzalez-Carreco, C. J. Serna, *J. Phys. D* **2003**, 36, R182.
- [15] a) Y. M. Huh, Y. W. Jun, H. T. Song, S. Kim, J. S. Choi, J. H. Lee, S. Yoon, K. S. Kim, J. S. Shin, J. S. Suh, J. Cheon, *J. Am. Chem. Soc.* **2005**, 127, 12387; b) H. T. Song, J. S. Choi, Y. M. Huh, S. Kim, Y. W. Jun, J. S. Suh, J. Cheon, *J. Am. Chem. Soc.* **2005**, 127, 9992.
- [16] M. Zachary, V. Chechik, *Angew. Chem.* **2007**, 119, 3368; *Angew. Chem. Int. Ed.* **2007**, 46, 3304.
- [17] a) D. V. Leff, P. C. O'Hara, J. R. Heath, W. M. Gelbart, *J. Phys. Chem.* **1995**, 99, 7036; b) M. J. Hostetler, S. J. Green, J. J. Stokes, R. W. Murray, *J. Am. Chem. Soc.* **1996**, 118, 4212; c) R. S. Ingram, M. J. Hostetler, R. W. Murray, *J. Am. Chem. Soc.* **1997**, 119, 9175; d) M. J. Hostetler, J. E. Wingate, C.-Z. Zhong, J. E. Harris, R. W. Vachet, M. R. Clark, J. D. Londono, S. J. Green, J. J. Stokes, G. D. Wignall, G. L. Glish, M. D. Porter, N. D. Evans, R. W. Murray, *Langmuir* **1998**, 14, 17; e) A. C. Templeton, M. J. Hostetler, C. T. Kraft, R. W. Murray, *J. Am. Chem. Soc.* **1998**, 120, 1906; f) M. J. Hostetler, A. C. Templeton, R. W. Murray, *Langmuir* **1999**, 15, 3782; g) M. J. Hostetler, A. C. Templeton, R. W. Murray, *Langmuir* **1999**, 15, 3782; h) A. C. Templeton, W. P. Wuefling, R. W. Murray, *Acc. Chem. Res.* **2000**, 33, 27; i) Y. Song, R. W. Murray, *J. Am. Chem. Soc.* **2002**, 124, 7096; j) A. Kassam, G. Bremner, B. Clark, G. Ulibarri, R. B. Lennox, *J. Am. Chem. Soc.* **2006**, 128, 3476.
- [18] a) M. Brust, A. Walker, D. Bethell, D. J. Schiffrin, R. Whyman, *J. Chem. Soc. Chem. Commun.* **1994**, 801; b) M. Brust, J. Fink, D. Bethell, D. J. Schiffrin, C. J. Kiely, *J. Chem. Soc. Chem. Commun.* **1995**, 1655.
- [19] a) L. Pasquato, P. Pengo, P. Scrimin, *J. Mater. Chem.* **2004**, 14, 3481; b) V. R. Reddy, *Synlett* **2006**, 1791.
- [20] M. Bartz, J. Küther, R. Seshadri, W. Tremel, *Angew. Chem.* **1998**, 110, 2646; *Angew. Chem. Int. Ed.* **1998**, 37, 2466.
- [21] a) K. Marubayashi, S. Takizawa, T. Kawakusu, T. Arai, H. Sasai, *Org. Lett.* **2003**, 5, 4409; b) S. Takizawa, M. L. Patil, K. Marubayashi, H. Sasai, *Tetrahedron* **2007**, 63, 6512; c) D. Jayaprakash, H. Sasai, *Tetrahedron: Asymmetry* **2001**, 12, 2589.
- [22] a) M. M. Alvarez, J. T. Khoury, T. G. Schaaf, M. N. Shafiqullin, I. Vezmar, R. L. Whetten, *J. Phys. Chem. B* **1997**, 101, 3706; b) R. L. Whetten, J. T. Khoury, M. M. Alvarez, S. Murthy, I. Vezmar, Z. L. Wang, P. W. Stephens, C. L. Cleveland, W. D. Luedtke, U. Landman, *Adv. Mater.* **1996**, 8, 428; c) W. D. Luedtke, U. J. Landman, *J. Phys. Chem. B* **1998**, 102, 6566; d) S. L. Logunov, T. S. Ahmadi, M. A. El-Sayed, J. T. Khoury, R. L. Whetten, *J. Phys. Chem. B* **1997**, 101, 3713.
- [23] M. Montalti, L. Prodi, N. Zaccheroni, R. Baxter, G. Teobaldi, F. Zerbetto, *Langmuir* **2003**, 19, 5172.
- [24] a) P. Ionita, A. Carageorghopol, B. C. Gilbert, V. Chechik, *J. Am. Chem. Soc.* **2002**, 124, 9048; b) P. Ionita, A. Carageorghopol, B. C. Gilbert, V. Chechik, *Langmuir* **2004**, 20, 11536.
- [25] T. Belser, M. Stöhr, A. Pfaltz, *J. Am. Chem. Soc.* **2005**, 127, 8720.
- [26] F. Ono, S. Kanemasa, J. Tanaka, *Tetrahedron Lett.* **2005**, 46, 7623.
- [27] M. J. Oila, A. M. P. Koskinen, *ARKIVOK* **2006**, 76.
- [28] H. Li, Y.-Y. Luk, M. Mrksich, *Langmuir* **1999**, 15, 4957.
- [29] T. Belser, E. N. Jacobsen, *Adv. Synth. Catal.* **2008**, 350, 967.
- [30] Y.-Y. Lin, S.-C. Tsai, S. J. Yu, *J. Org. Chem.* **2008**, 73, 4920.
- [31] B. S. Lee, S. K. Namgoong, S.-G. Lee, *Tetrahedron Lett.* **2005**, 46, 4501.
- [32] a) Z. Yinghuai, L. Kuijin, N. Huimin, L. Chuanzhao, L. P. Stubbs, C. F. Siong, T. Muihua, S. C. Peng, *Adv. Synth. Catal.* **2009**, 351, 2650; b) C. Ce, W. Li, S. Lin, J. Chen, J. Zheng, J.-C. Wu, Q. Zheng, G. Zhang, B. Jiang, *Chem. Commun.* **2009**, 5990.
- [33] a) J. Rockenberger, J. Scher, A. P. Alivisatos, *J. Am. Chem. Soc.* **1999**, 121, 11595; b) T. Hyeon, S. S. Lee, J. Park, Y. Chung, H. B. Na, *J. Am. Chem. Soc.* **2001**, 123, 12798; c) S. Sun, H. Zeng, *J. Am. Chem. Soc.* **2002**, 124, 8204; d) T. Hyeon, *Chem. Commun.* **2003**, 927; e) Y. Lee, J. Lee, C. J. Bae, J.-G. Park, H.-J. Noh, J.-H. Park, T. Hyeon, *Adv. Funct. Mater.* **2005**, 15, 503.
- [34] J. Jin, T. Iyoda, C. Cao, Y. Song, L. Jiang, T. J. Li, D. B. Zhu, *Angew. Chem.* **2001**, 113, 2193; *Angew. Chem. Int. Ed.* **2001**, 40, 2135.
- [35] T.-J. Yoon, W. Lee, Y.-S. Oh, J.-K. Lee, *New J. Chem.* **2003**, 27, 227.
- [36] M. H. Sousa, F. A. Tourinho, J. Depeyrot, G. J. da Silva, M. S. F. L. Lara, *J. Phys. Chem. B* **2001**, 105, 1168.
- [37] a) S. C. Bourque, F. Maltais, W. J. Xiao, O. Tardif, H. Alper, P. Arya, L. E. Manzer, *J. Am. Chem. Soc.* **1999**, 121, 3035; b) S. C. Bourque, H. Alper, *J. Am. Chem. Soc.* **2000**, 122, 956; c) J.-K. Lee, T.-J. Yoon, Y. K. Chung, *Chem. Commun.* **2001**, 1164; d) T. Malmstroem, H.

- Weigl, C. Andersson, *Organometallics* **1995**, *14*, 2593; e) K. Nozaki, Y. Itoi, F. Shibahara, E. Shirakawa, T. Ohta, H. Takaya, T. Hiyama, *J. Am. Chem. Soc.* **1998**, *120*, 4051.
- [38] a) A. Hu, G. T. Yee, W. Lin, *J. Am. Chem. Soc.* **2005**, *127*, 12486; b) G. Chouhan, D. Wang, H. Alper, *Chem. Commun.* **2007**, 4809.
- [39] Y. Sahoo, H. Pizem, T. Fried, D. Golodnitsky, L. Burstein, C. N. Sukeinik, G. Markovich, *Langmuir* **2001**, *17*, 7907.
- [40] R. Huisgen, *Pure Appl. Chem.* **1989**, *61*, 613.
- [41] a) C. W. Tornøe, M. Meldal in *American Peptide Symposium* (Eds.: M. Lebl, R. A. Houghten), Kluwer Academic, San Diego, **2001**, p. 263; b) V. V. Rostovtsev, L. G. Green, V. V. Fokin, K. B. Sharpless, *Angew. Chem.* **2002**, *114*, 2708; *Angew. Chem. Int. Ed.* **2002**, *41*, 2596; c) C. W. Tornøe, C. Christensen, M. Meldal, *J. Org. Chem.* **2002**, *67*, 3057.
- [42] a) P. D. Stevens, J. Fan, H. M. R. Gardimalla, M. Yen, Y. Gao, *Org. Lett.* **2005**, *7*, 2085; b) P. D. Stevens, G. Li, J. Fan, M. Yen, Y. Gao, *Chem. Commun.* **2005**, 4435; c) Y. Zheng, P. D. Stevens, Y. Gao, *J. Org. Chem.* **2006**, *71*, 537.
- [43] J. Jang, H. Ha, *Langmuir* **2002**, *18*, 5613.
- [44] T. Arai, T. Sato, H. Kanoh, K. Kaneko, K. Oguma, A. Yanagisawa, *Chem. Eur. J.* **2008**, *14*, 882.
- [45] Review: W. A. Herrmann, *Angew. Chem.* **2002**, *114*, 1342; *Angew. Chem. Int. Ed.* **2002**, *41*, 1290.
- [46] J.-W. Byun, Y.-S. Lee, *Tetrahedron Lett.* **2004**, *45*, 1837.
- [47] T. Rajh, L. X. Chen, K. Lukas, T. Liu, M. C. Thurnauer, D. M. Tiede, *J. Phys. Chem. B* **2002**, *106*, 10543.
- [48] C. Xu, K. Xu, H. Gu, R. Zheng, H. Liu, X. Zhang, Z. Guo, B. Xu, *J. Am. Chem. Soc.* **2004**, *126*, 9938.
- [49] a) B. Baruwati, K. M. Reddy, S. V. Manorama, R. K. Singh, O. Parkash, *Appl. Phys. Lett.* **2004**, *85*, 2833; b) D. Guin, B. Baruwati, S. V. Manorama, *J. Mol. Catal. A* **2005**, *242*, 26; c) D. Guin, B. Baruwati, S. V. Manorama, *Org. Lett.* **2007**, *9*, 1419.
- [50] R. Raja, B. V. Glovko, M. J. Thomas, A. Berenguer-Murcia, W. Zhou, S. Xie, G. F. B. Johnson, *Chem. Commun.* **2005**, 2026.
- [51] a) V. Polshettiwar, B. Baruwati, R. S. Varma, *Green Chem.* **2009**, *11*, 127; b) V. Polshettiwar, R. S. Varma, *Chem. Eur. J.* **2009**, *15*, 1582; c) V. Polshettiwar, R. S. Varma, *Org. Biomol. Chem.* **2009**, *7*, 37.
- [52] O. Gleeson, R. Tekoriute, Y. K. Gun'ko, S. J. Connon, *Chem. Eur. J.* **2009**, *15*, 5669.
- [53] C. Duanmu, I. Saha, Y. Zheng, B. M. Goodson, Y. Gao, *Chem. Mater.* **2006**, *18*, 5973.
- [54] a) J. Lim, E. E. Simanek, *Mol. Pharm.* **2005**, *2*, 273; b) W. Zhang, E. E. Simanek, *Org. Lett.* **2000**, *2*, 843.
- [55] J. Park, K. An, Y. Hwang, J.-G. Park, H.-J. Noh, J.-Y. Kim, J.-H. Park, N.-M. Hwang, T. Hyeon, *Nat. Mater.* **2004**, *3*, 891.
- [56] D. Rosario-Amorin, X. Wang, M. Gaboyard, R. Clérac, S. Nlate, K. Heuzé, *Chem. Eur. J.* **2009**, *15*, 12636.
- [57] a) Y. Yu, Y. Yin, B. T. Mayers, Y. Xia, *Nano Lett.* **2002**, *2*, 183; b) N. Kohler, G. E. Fryxell, M. Zhang, *J. Am. Chem. Soc.* **2004**, *126*, 7206.
- [58] a) G. Lu, W. Mai, R. Jin, L. Gao, *Synlett* **2008**, 1418; b) M.-J. Jin, D.-H. Lee, *Angew. Chem.* **2010**, *122*, 1137; *Angew. Chem. Int. Ed.* **2010**, *49*, 1119.
- [59] a) S. Ding, Y. Xing, M. Radosz, Y. Shen, *Macromolecules* **2006**, *39*, 6399; b) H. Tang, M. Radosz, Y. Shen, *Macromol. Rapid Commun.* **2006**, *27*, 1127.
- [60] a) M. Kato, M. Kamigaito, M. Sawamoto, T. Higashimura, *Macromolecules* **1995**, *28*, 1721; b) J. S. Wang, K. Matyjaszewski, *J. Am. Chem. Soc.* **1995**, *117*, 5614.
- [61] A.-H. Lu, W. C. Li, A. Kiefer, W. Schmidt, E. Bill, G. Fink, F. Schüth, *J. Am. Chem. Soc.* **2004**, *126*, 8616.
- [62] D. K. Yi, S. S. Lee, J. Y. Ying, *Chem. Mater.* **2006**, *18*, 2459.
- [63] R. Narayanan, M. A. El-Sayed, *J. Phys. Chem. B* **2004**, *108*, 8572.
- [64] S. Ceylan, C. Friese, C. Lammel, K. Mazac, A. Kirschning, *Angew. Chem.* **2008**, *120*, 9083; *Angew. Chem. Int. Ed.* **2008**, *47*, 8950.
- [65] R. Abu-Reziq, H. Alper, D. Wang, M. L. Post, *J. Am. Chem. Soc.* **2006**, *128*, 5279.
- [66] a) S. M. Lu, H. Alper, *J. Am. Chem. Soc.* **2003**, *125*, 13126; b) P. Arya, G. Panda, N. V. Rao, H. Alper, S. C. Bourque, L. E. Manzer, *J. Am. Chem. Soc.* **2001**, *123*, 2889; c) S. C. Bourque, H. Alper, L. E. Manzer, P. Arya, *J. Am. Chem. Soc.* **2000**, *122*, 956.
- [67] See, for example: a) M. Kawamura, K. Sato, *Chem. Commun.* **2006**, 4718; b) S. Luo, X. Zheng, J.-P. Cheng, *Chem. Commun.* **2008**, 5719; c) X. Zheng, S. Luo, L. Zhang, J.-P. Cheng, *Green Chem.* **2009**, *11*, 455; d) V. Polshettiwar, B. Baruwati, R. S. Varma, *Chem. Commun.* **2009**, 1837.
- [68] C. A. Dalaigh, S. A. Corr, Y. Gun'ko S. J. Connon, *Angew. Chem.* **2007**, *119*, 4407.
- [69] S. Luo, X. Zheng, H. Xu, X. Mi, L. Zhang, J.-P. Cheng, *Adv. Synth. Catal.* **2007**, *349*, 2431.
- [70] J. Li, Y. Zhang, D. Han, Q. Gao, C. Li, *J. Mol. Catal. A* **2009**, *298*, 31.
- [71] A. Schätz, M. Hager, O. Reiser, *Adv. Funct. Mater.* **2009**, *19*, 2109.
- [72] S. Sun, H. Zeng, *J. Am. Chem. Soc.* **2002**, *124*, 8204.
- [73] N. Wu, L. Fu, M. Su, M. Aslam, K. C. Wong V. P. Dravid, *Nano Lett.* **2004**, *4*, 383.
- [74] F. Michalek, A. Lagunas, C. Jimeno, M. A. Pericàs, *J. Mater. Chem.* **2008**, *18*, 4692.
- [75] L. M. Liz-Marzán, M. Giersig, P. Mulvaney, *Chem. Commun.* **1996**, 731.
- [76] A. H. Lu, E. L. Salabas, F. Schüth, *Angew. Chem.* **2007**, *119*, 1242; *Angew. Chem. Int. Ed.* **2007**, *46*, 1222.
- [77] a) Y. Saito, *Carbon* **1995**, *33*, 979; b) J. H. J. Scott, S. A. Majetich, *Phys. Rev. B* **1995**, *52*, 12564; c) J. Jiao, S. Seraphin, X. Wang, J. C. Withers, *J. Appl. Phys.* **1996**, *80*, 103.
- [78] a) Z. H. Wang, C. J. Choi, B. K. Kim J. C. Kim, Z. D. Zhang, *Carbon* **2003**, *41*, 1751; b) E. Flahaut, F. Agnoli, J. Sloan, C. O'Connor, M. L. H. Green, *Chem. Mater.* **2002**, *14*, 2553.
- [79] a) Y. Lu, Z. Zhu, Z. Liu, *Carbon* **2005**, *43*, 36; b) N. Sano, H. Akazawa, T. Kikuchi, T. Kanki, *Carbon* **2003**, *41*, 2159; c) J. Nishijo, C. Okabe, O. Oishi, N. Nishi, *Carbon* **2006**, *44*, 2943.
- [80] a) R. N. Grass, E. K. Athanassiou, W. J. Stark, *Angew. Chem.* **2007**, *119*, 4996; *Angew. Chem. Int. Ed.* **2007**, *46*, 4909; b) I. K. Herrmann, R. N. Grass, D. Mazunin, W. J. Stark, *Chem. Mater.* **2009**, *21*, 3275; c) R. N. Grass, W. J. Stark, *J. Mater. Chem.* **2006**, *16*, 1825.
- [81] W. J. Stark, L. Madler, M. Maciejewski, S. E. Pratsinis, A. Baiker, *Chem. Commun.* **2003**, 588.
- [82] a) F. M. Koehler, M. Rossier, M. Waelle, E. K. Athanassiou, L. K. Limbach, R. N. Grass, D. Günther, W. J. Stark, *Chem. Commun.* **2009**, 4862; b) M. Rossier, F. M. Koehler, E. K. Athanassiou, R. N. Grass, B. Aeschlimann, D. Günther, W. J. Stark, *J. Mater. Chem.* **2009**, *19*, 8239.
- [83] a) C. G. Tan, R. N. Grass, *Chem. Commun.* **2008**, 4297; b) R. Fuhrer, E. K. Athanassiou, N. A. Luechinger, W. J. Stark, *Small* **2009**, *5*, 383.
- [84] A. Schätz, R. N. Grass, W. J. Stark, O. Reiser, *Chem. Eur. J.* **2008**, *14*, 8262.
- [85] K. Hata, H. Fujihara, *Chem. Commun.* **2002**, 2714.
- [86] A. Schätz, R. N. Grass, Q. Kainz, W. J. Stark, O. Reiser, *Chem. Mater.* **2010**, *22*, 305.
- [87] a) E. Katz, *J. Electroanal. Chem.* **1994**, *365*, 157; b) H. Jaegfeldt, T. Kuwana, G. Johansson, *J. Am. Chem. Soc.* **1983**, *105*, 1805; c) R. J. Chen, Y. Zhang, D. Wang, H. Dai, *J. Am. Chem. Soc.* **2001**, *123*, 3838.
- [88] S. Wittmann, A. Schätz, R. N. Grass, W. J. Stark, O. Reiser, *Angew. Chem.* **2010**, *122*, 1911; *Angew. Chem. Int. Ed.* **2010**, *49*, 1876.
- [89] L. K. Limbach, Y. Li, R. N. Grass, T. J. Brunner, M. A. Hintermann, M. Müller, D. Gunther, W. J. Stark, *Environ. Sci. Technol.* **2005**, *39*, 9370.
- [90] Y. Kobayashi, M. Horie, M. Konno, B. Rodriguez-Gonzalez, L. M. Liz-Marzán, *J. Phys. Chem. B* **2003**, *107*, 7420.
- [91] a) N. S. Sobal, M. Hilgendorff, H. Moehwald, M. Giersig, M. Spasova, T. Radetic, M. Farle, *Nano Lett.* **2002**, *2*, 621; b) M. Chen, S. Yamamuro, D. Farrell, S. A. Majetich, *J. Appl. Phys.* **2003**, *93*, 7551.
- [92] a) A.-H. Lu, W. Li, N. Matoussevitch, B. Spliethoff, H. B. Penne-mann, F. Schüth, *Chem. Commun.* **2005**, 98; b) M. Chen, S. Yamamuro, D. Farrell, S. A. Majetich, *J. Appl. Phys.* **2003**, *93*, 7551.
- [93] a) L. E. Euliss, S. G. Grancharov, S. O'Brien, T. J. Deming, G. D. Stucky, C. B. Murray, G. A. Held, *Nano Lett.* **2003**, *3*, 1489; b) X.

- Liu, Y. Guan, Z. Ma, H. Liu, *Langmuir* **2004**, *20*, 10278; c) R. Hong, N. O. Fischer, T. Emrick, V. M. Rotello, *Chem. Mater.* **2005**, *17*, 4617; d) M. Kim, Y. Chen, Y. Liu, X. Peng, *Adv. Mater.* **2005**, *17*, 1429.
- [94] a) A. G. M. Barrett, B. T. Hopkins, J. Köbberling, *Chem. Rev.* **2002**, *102*, 3301; b) J. Lu, P. H. Toy, *Chem. Rev.* **2009**, *109*, 815.
- [95] E. de Jesus, J. C. Flores, *Ind. Eng. Chem. Res.* **2008**, *47*, 7968.
- [96] a) H. M. R. Gardimalla, D. Mandal, P. D. Stevens, M. Yen, Y. Gao, *Chem. Commun.* **2005**, 4432; b) P. Pengo, S. Polizzi, L. Pasquato, P. Scrimin, *J. Am. Chem. Soc.* **2005**, *127*, 1616; c) F. Manea, F. B. Houillon, L. Pasquato, P. Scrimin, *Angew. Chem.* **2004**, *116*, 6291; *Angew. Chem. Int. Ed.* **2004**, *43*, 6165; d) R. Bonomi, F. Selvestrel, V. Lombardo, C. Sissi, S. Polizzi, F. Mancin, U. Tonellato, P. Scrimin, L. Bromberg, T. A. Hatton, *Ind. Eng. Chem. Res.* **2005**, *44*, 7991.

Received: December 17, 2009  
Published online: July 19, 2010